



BRNO UNIVERSITY OF TECHNOLOGY

VYSOKÉ UČENÍ TECHNICKÉ V BRNĚ

FACULTY OF ELECTRICAL ENGINEERING AND COMMUNICATION

FAKULTA ELEKTROTECHNIKY
A KOMUNIKAČNÍCH TECHNOLOGIÍ

DEPARTMENT OF POWER ELECTRICAL AND ELECTRONIC ENGINEERING

ÚSTAV VÝKONOVÉ ELEKTROTECHNIKY A ELEKTRONIKY

INVESTIGATION ON OPERATING CHARACTERISTICS OF MULTI-PHASE MACHINE

STUDIE PRACOVNÍCH CHARAKTERISTIK VÍCE-FÁZOVÉHO STROJE

MASTER'S THESIS
DIPLOMOVÁ PRÁCE

AUTHOR
AUTOR PRÁCE

Bc. Kristián Kuna

SUPERVISOR
VEDOUCÍ PRÁCE

Ing. Jan Bárta, Ph.D.

BRNO 2020

Master's Thesis

Master's study field **Power Electrical and Electronic Engineering**

Department of Power Electrical and Electronic Engineering

Student: Bc. Kristián Kuna

ID: 186440

**Year of
study:** 2

Academic year: 2019/20

TITLE OF THESIS:

Investigation on operating characteristics of multi-phase machine

INSTRUCTION:

1. The current state of the art review of a multiphase electrical machine.
2. Theoretical study of the multiphase electrical machines concerning geometry/winding choice and control.
3. Analytical analysis of properties of the multiphase electrical machines.
4. Extended analysis of a selected multiphase electrical machine using finite element methods.

RECOMMENDED LITERATURE:

- [1] PYRHONEN, J.; JOKINEN t.; HRABOVCOVÁ V. Design of rotating eletrical machines. John Wiley and Sons, 2007. ISBN 978-0-470-69516-6.
- [2] J.R. HENDERSHOT, T.J.E. MILLER . Design of Brushless Permanent-Magnet Machines. Motor Design Books LLC; Second Edition edition, 2010. ISBN 978-0984068708.
- [3] A. E. Fitzgerald, Ch. Kingsley, S. Umans "Electric Machinery", McGraw-Hill Companies Inc., 2003. 688 s. ISBN 0-07-112193-5

**Date of project
specification:** 3.2.2020

Deadline for submission: 1.6.2020

Supervisor: Ing. Jan Bárta, Ph.D.

doc. Ing. Ondřej Vitek, Ph.D.
Subject Council chairman

WARNING:

The author of the Master's Thesis claims that by creating this thesis he/she did not infringe the rights of third persons and the personal and/or property rights of third persons were not subjected to derogatory treatment. The author is fully aware of the legal consequences of an infringement of provisions as per Section 11 and following of Act No 121/2000 Coll. on copyright and rights related to copyright and on amendments to some other laws (the Copyright Act) in the wording of subsequent directives including the possible criminal consequences as resulting from provisions of Part 2, Chapter VI, Article 4 of Criminal Code 40/2009 Coll.

Abstrakt

S postupem času se elektrotechnický průmysl posouval dopředu. Přišel rozvoj v automobilovém průmyslu, leteckém průmyslu, navigaci a dalších odvětví. S rozvojem automobilového a leteckého průmyslu se zvětšila potřeba pro motory s vysokou spolehlivostí. Samotný fakt zapříčinil rozvoj motorů s více fázemi. Tyto stroje mají za úkol zvýšit spolehlivost, ale zároveň zachovat nebo zvýšit výkon stroje.

Klíčová slova

5-fázové stroje, 3-fázové stroje, analytický návrh, porovnání strojů, rekonfigurace proudů, Lagrangové multiplikátory

Abstract

In recent decades, the electrical industry has been rapidly developed. The development is in electrical vehicles, navigation, electrical aircraft, high-power wind generators, multi-phase electrical machines and drivers. With development in the automotive industry and airspace industry, the need of high-reliability electrical machines. This fact results in the development of poly-phase machines. These machines try to achieve a higher reliability with the same or higher power rating.

Keywords

5-phase machines, 3-phase machines, analytical design, comparison of the machines, reconfiguration of currents, Lagrange multipliers

Rozšířený abstrakt

Tato práce je zaměřená na více-fázové stroje. Je rozdělena do čtyř částí. V první části je zaměřena na aktuální stav poznání o více-fázových strojích. Je tam popisováno využití 5 fázového stroje jako generátoru pro větrné turbíny, jako pohonu pro elektrické letadlo nebo také pro aplikaci přímého připojení motoru na kolo v automobilovém průmyslu. Taktéž je v první kapitole popsáno řízení více-fázových strojů pomocí SVM. Dále jsou tam uvedeny možnosti rozložení statorového vinutí pro více-fázové stroje. Na závěr této kapitoly jsou uvedeny některé možnosti (spůsoby) testování více-fázových strojů.

Druhá kapitola začíná výpočty pro druh vinutí u tří a pěti fázových strojů. Jsou tam uvedeny výpočty pro stabilitu vynutí pro jednotlivé případy. Jednotlivé výsledky jsou uvedeny v tabulkách 2.1, 2.2, 2.3 a 2.4. Dalším krokem této kapitoly je srovnání tří a pěti-fázových indukčních strojů. Je tam uvedeno několik variant pro pěti-fázový stroj. Všechny stroje byly navrženy tak, aby měly stejný výkon, fázové napětí, rozměry stroje a počet pólů. Všechny parametry strojů jsou uvedeny v Tab. 2.5. Následně bylo provedeno srovnání pro jednotlivé případy. Porovnávaly se například Joulovy stráty ve statoru a rotoru, jejich účinnost a účinník. Všechny hodnoty jsou vidět v Tab. 2.6.

Na začátku třetí kapitoly je uvedený postup návrhu pěti-fázového stroje pomocí matematické analýzy. V tomto návrhu je také poukázáno na fakt, že u pěti-fázového stroje vytváří třetí harmonická přídavný moment a proto je požitá i ve výpočtech. Následně jsou spomenuty chybné stavy stroje. Blíže rozebrané jsou stavy kdy se nesepe jedna nebo dvě fáze a tedy jednou nebo dvěma fázemi neprotéká žádný proud. Pro tyto případy byly vypočítané průběhy proudů za pomoci Lagrangových multiplikátorů. Tyto průběhy měly za účel dosáhnout požadovaný moment v případě, kdy dojde k výpadku jedné nebo dvou fází. Dále byly také uvedeny jiné možnosti rekonfigurace proudů ve stroji, jako například genetický algoritmus.

Ve čtvrté a poslední části byla provedena konečně prvková analýza. Parametry stroje jsou uvedeny v Tab. 4.1. Analýza byla provedena pro čtyři případy. První byl chod naprázdno, kdy se získaly hodnoty indukovaného napětí stroje, které byly použity pro výpočet rekonfigurace proudů pro jednotlivé případy. V prvním případě se jednalo o chod pod zatížením, kdy byla provedena rekonfigurace tak, aby se dosáhlo hodnoty momentu 10 Nm. Dosažený moment stroje byl 10.1 Nm. Následně se provedla konečně prvková analýza i pro chybové stavy. V těchto případech se hodnoty požadovaného momentu snižovaly, aby se amplitudy proudů držely v blízkosti chodu stroje při normálních podmínkách. Hodnoty momentu byly sníženy na 8 Nm pro případ poruchy v jedné fázi a 6 Nm pro případ výpadku ve dvou fázích.

Bibliographic citation

KUNA, Kristián. Investigation on operating characteristics of multi-phase machine. Brno, 2020. Dostupné také z: <https://www.vutbr.cz/studenti/zav-prace/detail/125797>. Master's Thesis. Vysoké učení technické v Brně, Fakulta elektrotechniky a komunikačních technologií, Department of Power Electrical and Electronic Engineering. Supervisor Jan Bárta.

Prohlášení

Prohlašuji, že svou diplomovou práci na téma „Investigation on operating characteristics of multi-phase machine“ jsem vypracoval samostatně pod vedením vedoucího diplomové práce a s použitím odborné literatury a dalších informačních zdrojů, které jsou všechny citovány v práci a uvedeny v seznamu literatury na konci práce.

Jako autor uvedené diplomové práce dále prohlašuji, že v souvislosti s vytvořením této diplomové práce jsem neporušil autorská práva třetích osob, zejména jsem nezasáhl nedovoleným způsobem do cizích autorských práv osobnostních a jsem si plně vědom následků porušení ustanovení § 11 a následujících autorského zákona č. 121/2000 Sb., včetně možných trestněprávních důsledků vyplývajících z ustanovení části druhé, hlavy VI. díl 4 Trestního zákoníku č. 40/2009 Sb.

V Brně dne 22. května 2019

Podpis autora

Poděkování

This work has been supported by the COMET-K2 Center of the Linz Center of Mechatronics (LCM) funded by the Austrian federal government and the federal state of Upper Austria.

I would like to express many thanks to my supervisors Ing. Jan Bárta, Ph.D. from Brno University of Technology. I am very grateful for all his problem solving ideas, patience, all the time he spent with me on our personal consultations.

I am also very grateful to Dipl.-Ing. Dr. Gerd Bramerdorfer from Johannes Kepler University in Linz to cooperation with me on my master thesis, for providing me with material background and support.

In Brno

Sign by Author

Contents

List of Figures	1
List of Tables	3
List of Symbols	3
Introduction	6
1 State of the art of poly-phase machines	7
1.1 Theory of the poly-phase machines	7
1.2 Five-phase permanent magnet generator	7
1.3 Propulsion of electric aircraft	8
1.4 Synchronous motor for in-wheel application	8
1.5 Space-Vector Modulation	8
1.5.1 Voltage Source Inverter (VSI) for five phase	9
1.6 Space-Vector Decomposition for five phase machine	11
1.6.1 Stator arrangements	11
1.6.2 VSD Full phase progression $360^\circ/m$	12
1.7 Testing of the five-phase machines	14
2 Comparison of five-phase and three-phase machines	15
2.1 Slot pole number	15
2.2 Performance comparison of poly-phase induction machines	18
3 Analytical methods of the five-phase machines	21
3.1 Mathematical model of the Five Phase PM motor	21
3.2 Short-circuit of five-phase machine	25
3.2.1 Short-circuit of one phase	25
3.2.2 Short-circuit of two phases	26
3.3 Open-circuit of five phase machine	26
3.3.1 Lagrange multipliers	27
3.3.2 Calculation of currents	28
3.3.3 Different method of calculation currents Genetic Algorithm	31
3.3.4 Different method of calculation currents On-line Optimal Current	36
4 Extended analysis by means of fine element methods	40
4.1 Motor under no-load	42
4.2 Motor under full-load	44
4.2.1 Sinusoidal back EMF	44

4.2.2	Back EMF from no-load.....	45
4.3	<i>One phase open</i>	47
4.4	<i>Two phases open</i>	49
	Conclusion	50
	References	52

List of Figures

Figure 1.1: Space Vector representation in d-q plane.	9
Figure 1.2: Space Vector representation in d3-q3 plane.	10
Figure 1.3: Symmetrical winding scheme for five phase (full progression).	12
Figure 1.4: Dual three-phase winding (half phase progression).	12
Figure 3.1: Stator winding [25].	22
Figure 3.2: Shift between phases [26].	26
Figure 3.3: Configuration of the windings. a) star, b) pentagon, c) pentacle.	29
Figure 3.4: All healthy phases (sinusoidal back EMF).	29
Figure 3.5: All healthy phases (non sinusoidal back EMF).	30
Figure 3.6: Reconfiguration one phase open (Phase A is open, 10 Nm).	31
Figure 3.7: Reconfiguration one phase open (Phase A is open, 8 Nm).	32
Figure 3.8: Reconfiguration two phases open (Phases A and B are open, 10 Nm).	33
Figure 3.9: Reconfiguration two phases open (Phases A and B are open, 8 Nm).	33
Figure 3.10: Reconfiguration two phases open (Phases A and C are open, 6 Nm).	34
Figure 3.11: Curves of currents with application of GA(6 parameters).	35
Figure 3.12: Torque with one phase open (6 parameters).	35
Figure 3.13: Torque with one phase open (12 parameters).	36
Figure 3.14: Optimal currents during normal operation.[27].	37
Figure 3.15: Optimal currents during open-phase circuited(one phase open).[27].	38
Figure 3.16: Optimal currents during open-phase circuited(one phase open).[27].	38
Figure 3.17: Optimal currents during open-phase circuited(two non- consecutive phase open) [27].	39
Figure 4.1: Geometry of the motor.	41
Figure 4.2: Back EMF(no-load).	42
Figure 4.3: Mesh of the half of the motor.	43
Figure 4.4: Induction under no-load.	43
Figure 4.5: Magnetic induction full-load.	44
Figure 4.6: Currents (Sinusoidal back EMF).	45
Figure 4.7: Torque 1500 rpm (sinusoidal back EMF).	45
Figure 4.8: Currents (no-load back EMF)	46
Figure 4.9: Torque 1500 rpm (no-load back EMF).	46

Figure 4.10: Torque 1500 rpm (one phase open, 10 Nm). 47
Figure 4.11: Currents (one phase open, 10 Nm). 48
Figure 4.12: Torque 1500 rpm (one phase open, 8 Nm). 48
Figure 4.13: Currents (one phase open, 8 Nm). 48
Figure 4.14: Currents (two phases open, 6 Nm). 49
Figure 4.15: Torque 1500 rpm (one phase open, 8 Nm). 49

List of Tables

Table 2.1: Number of slot per pole per phase five-phase.	15
Table 2.2: Stable/unstable winding for five-phase.	16
Table 2.3: Number of slot per pole per phase three-phase.	16
Table 2.4: Stable/unstable winding for three-phase.	17
Table 2.5: Rating and dimensions of machines [23]	18
Table 2.6: Performance comparison of the three and five phase machines [23].	19
Table 3.1: Values of parameter using GA optimization(six parameters) [30].	33
Table 3.2: Values of parameter using GA optimization(12 parameter funda- mental) [30].	35
Table 3.3: Values of parameter using GA optimization(12 parameters third harmonic) [30].	35
Table 3.4: Values of torque in each of the open phase scenarios(On-Line method).38	
Table 3.5: Values of Joule losses in each of the open phase scenarios(On-Line method).	39
Table 4.1: Parameters of the motor.	40
Table 4.2: Measured maximal values of magnetic induction of the motor	42
Table 4.3: Calculated maximal values of magnetic induction of the motor (Full-load).	46

List of symbols and acronyms

SVM	Space-Vector modulation	[-]
VSI	Voltage Source Inverter	[-]
EESG	Electrically excited synchronous generators	[-]
PMSG	Permanent magnet synchronous generators	[-]
EA	Electrical aircraft	[-]
IPMM	Interior permanent magnet motors	[-]
SPMM	Interior permanent magnet motors	[-]
PMSRM	Permanent magnet assisted synchronous reluctance motors	[-]
v_{pn}	voltage between the star point and negative dc bus	[V]
VSD	Space-Vector Decomposition	[-]
m	Number of phases	[-]
PM	Permanent Magnet	[-]
S	Number of slots	[-]
p	Number of poles	[-]
GCD	Greatest common division	[-]
k_p	Pitch factor	[-]
k_d	Distribution factor	[-]
v	Number of harmonic	[-]
α_u	Slot angel	[°]
q	Number of slots per pole per phase	[-]
y	Step of winding	[-]
y_q	Coil span	[-]
V_S	Stator voltage	[V]
R_S	Stator resistance	[Ω]
I_S	Stator current	[A]
Ψ_S	Stator flux linkage	[Wb]
L_{SS}	Stator inductance	[H]
Ψ_m	Permanent magnet flux linkage	[Wb]
Ψ_{m1}	First harmonic amplitude	[Wb]
Ψ_{m3}	Third harmonic amplitude	[Wb]
θ_r	Rotor position	[°]
N_a	Winding function for phase a	[-]
ϕ	Spatial angel	[rad]
N_s	Number of turns	[-]
$T(\theta_r)$	Transformation matrix	[-]
W_{CO}	Co-energy	[J]
T	Torque	[Nm]
GA	Genetic algorithm	[-]

OC	On-line optimal current	[-]
LM	Lagrange multipliers	[-]
H	Vector of ones	[-]
P_w	Wanted power output	[W]
P_{out}	Output power	[W]
λ_1	Lagrange multiplier	[-]
λ_2	Lagrange multiplier	[-]
P_{cu}	Joule losses	[W]
n	Number of healthy phases	[-]
β_1	Phase shift, fundamental	[rad]
m_1	Multiplexer of amplitude, fundamental	[-]
β_{b3}	Phase shift, third harmonic	[rad]
m_{b3}	Multiplexer of amplitude, third harmonic	[-]
e	Back electromotive force	[V]
ε	Speed normalized back electromotive force	[V]
A	Criterion	[-]
ε_{acc}	Accessible back electromotive force	[V]
ε_z	Zero-sequence component of ε	[V]
ε_{12}	Speed normalized back electromotive force of phases 1 and 2	[V]
Q	Number of stator slots	[-]
p_r	Number of rotor pole-pair	[-]
FEA	Finite elements analyzes	[-]
IPM	Interior permanent magnets	[-]
EMF	Electromotive force	[-]

Introduction

In recent decades, the electrical industry has been rapidly developed. The development is in electrical vehicles, navigation, electrical aircraft, high-power wind generators, multi-phase electrical machines and drivers. With development in the automotive industry and aerospace industry, the need of high-reliability electrical machines. This fact comes with wide attention for multi-phase machines. The new structures of combining multi-phase winding with new techniques, new topology and optimization for pursuing high-reliability applications. After individual models have been created for normal and fault conditions. Those models are used to analyze the characteristics of those multi-phase machines.

This thesis will be investigating the multi-phase machines. First part will be divided into four sections. In the first section the theory of poly-phase machines will be introduced, their design, operating of the machines and testing. In the second section, the comparison of the five-phase and three-phase machines are mentioned. Such as slot pole number and his impact on the machine and comparison of the performance of three and five-phase machines. In the third section of the first part, the analytical methods of five-phase machines are introduced. Such as the mathematical model of five-phase permanent magnet motor, the calculation of torque injection of third harmonic current and his impact. Also short-circuit variants are mentioned. For cases of only one phase is shorted, two consecutive phases or two non-consecutive phases. Subsequently there are cases of open phases in the third chapter.

In the final final and four chapter there is a model of five-phase machine with cases of open phase circuited. With the impact on the torque of the machine. This analyzation was done in Ansys Maxwell.

1 State of the art of poly-phase machines

1.1 Theory of the poly-phase machines

This chapter is dealing with poly-phase machines. As a multiplex machines will be considered machines, which have some phase multiple by a number of two, three etc.. Simultaneously, as poly-phase machines can be considered five, seven or more phase machines. The application of poly-phase machines is interesting for such a reason as that the power conversion could be split into smaller units and therefore for the very large machines could be more efficient and/or more economical to use n number of invertors with 1/nth rating, instead of one large inventor with the full rating. With a greater number of inverters then 1 (in our case n) the possibility of working, even if a malfunction occur or the inverter is switched off [1].

The term of multi-phase suggests an intention of tolerance when malfunction appear and function of independent channels, whereby the machine is still capable to operate[1]. The machines are capable of functioning in open case scenarios, since they still can generate a rotating field. But it is need to be carefully considered, because it can have an impact on other parts of the machine. Also some kind of strategy needs to be implemented for this cases such as in [2], [3], [4] and [5]. Also, their control strategy needs to be discussed such as space-vector modulation.

Poly-phase electrical machines can be used such as permanent magnets generators for a wind turbines [6], propulsion for an electric aircraft [7] or synchronous motor for in-wheel applications. Each of this cases will be describe closer [8].

1.2 Five-phase permanent magnet generator

With raising number of well priced permanent magnets with great parameters, the interest of using PM in construction of electric machines raised as well. One of the application place is in in five-phase PM generator, which is used as a wind turbine. Many types of wind turbine generators systems have been developed to achieve a higher amount of capture energy. From [6] those systems are electrically exited synchronous generators (EESG) or permanent magnet synchronous generators (PMSG).

With direct-drive permanent magnet generators come some advantages such as lower failure rate and higher energy yield, but it also comes with disadvantages such as demagnetization of PM at higher temperature, the cost of PM (the price is better, but still relatively high) or incapability of controlling the field strength. By applying of the five phases for generators and dividing the necessary power into a five phases, a higher density of power can be obtained [6], [9] and [10]. Different PM types such as alnico PM, ferrits, samarium-cobalt or neodymium-iron-boron PM in PMSG can be found in [6].

1.3 Propulsion of electric aircraft

As well as PM, the energy storage systems have been enhanced. This enhancements lead to a higher interest in the electrical aircraft (EA), especially as an electric propulsion [7]. The trend is to replace the hydraulic systems with an electrical actuators, which are fed from an electric generators. These generators are coupled with gas turbine or the engine of the aircraft. Some of the publications for EA propose the hybridization of the propulsion systems such as in [11] and [12].

The electric propulsion system for EA needs to be reliable and have fault-tolerant characteristics. This means that the EA still capable of driving, even if the fault occurs. Example of the reconfiguration can be seen in [5] and [3]. For this reason, the electric motor, which is used to have a higher number of phases. In [7] is proposed two solutions for the five-phase machine. The EA has two electric motors. One has a higher degree of fault tolerance but at the same increasing the total amount of weight. This solution has two VSI. Each motor has its own VSI. On the other hand, the second solution with just one VSI is a solution with lower weight but in case of fault state, this solution reduces the number of phases in both motors.

1.4 Synchronous motor for in-wheel application

Over the years the use of electric motors in vehicles grown (electric vehicles or hybrid electric vehicles). Some of the solutions are brushless DC PM motors, interior permanent magnets motors (IPMM) and surface mounted PM motors (SPMM) [8], [13].

One of the alternatives to the IPMM and SPMM is multi-phase permanent magnet assisted synchronous reluctance motors (PMSRM). Multi-phase PMSRM have better performance compared to SPMM and IPMM [13]. Also, other advantages of the multi-phase PMSRM are that, the fault tolerance capability is increased and torque ripple is decreased.

Now if we take a look at the differences in PMSRM internal and external rotor configuration. In case of the internal rotor, the motor is used as a boost for the engine torque but the disadvantages that the rotor needs to be coupled with gears and complex power train. Nonetheless the second case with external rotor for PMSRM does not need the complex coupling in the power train [13], [14], [15].

1.5 Space-Vector Modulation

Space-Vector modulation (SVM) for the five-phase machine is using a sinusoidal voltage as a phasor. The second option is an amplitude vector which is rotating at an angular frequency (angular frequency is a constant). The inverter which is used for five-phase machines have a 32 internal states (2^n in case of five phases 2^5). This 32 vector can be split into non-zero and zero. Thirty of these vectors are non-zero and two zero vectors[16].

If it is used a d-q transformation with five outputs of voltage, it will shape two times 32 space vectors. As it is developed into two representation of space vector, one of them will be a d-q and the second will be described as a d3-q3. These representations can be seen in Figure 1.4 and 1.5.

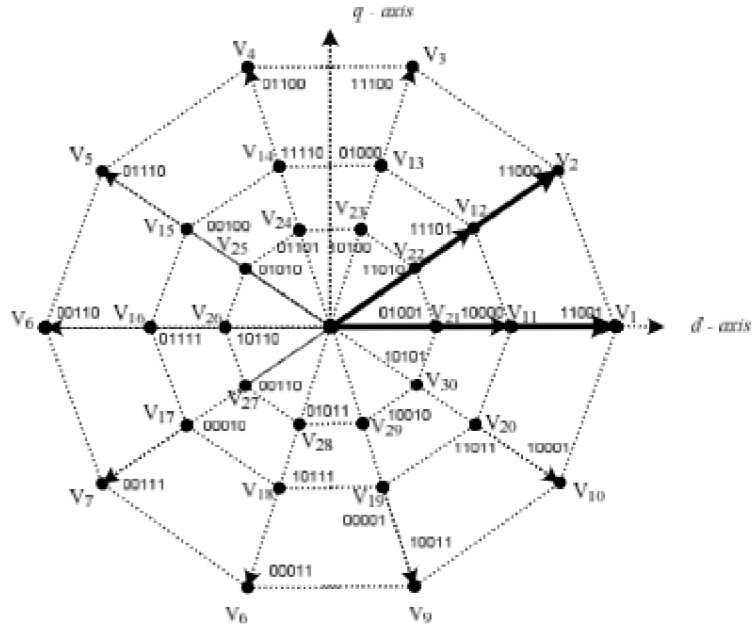


Figure 1.1: Space Vector representation in d-q plane.

As can be seen from Figure 1.4 and 1.5 the outer part of the d-q plane is shown as a most inside hexagon of d3-q3. However, the middle part of each d-q and d3-q3 plane are placed into the same region.

1.5.1 Voltage Source Inverter (VSI) for five phase

The five-phase is power from an inverter, which have circuit consists of two power devices. This power devices are semiconductors and are in antiparallel connection. By using a space vector form is crated a model of VSI for five-phase. In this model are assumed [16]:

- Ideal commutation
- Zero voltage drops

Five phase machine is connected in a star configuration. Now the phase to voltage of the star configuration is wanted. This voltage can be easy to find, if we define the voltage between the star point and the negative dc bus (v_{pn}) [16].

From this assumption can be defined voltage for each phase [16].

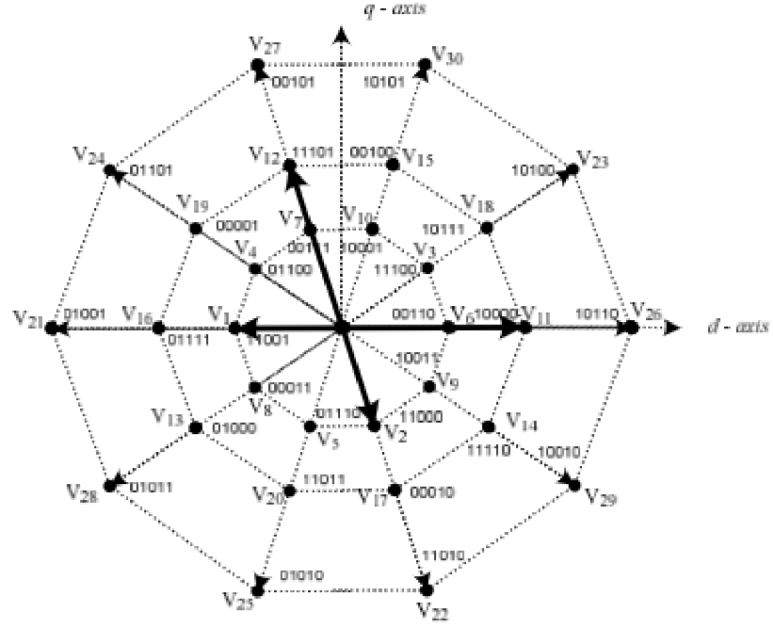


Figure 1.2: Space Vector representation in d3-q3 plane.

$$v_A = v_a + v_{pn}$$

$$v_B = v_b + v_{pn}$$

$$v_C = v_c + v_{pn}$$

$$v_D = v_d + v_{pn}$$

$$v_E = v_e + v_{pn}$$

Because of phase voltage sum is equal to zero, for star connection. The equation for v_{pn} occur [16].

$$v_{pn} = \frac{1}{5}(v_A + v_B + v_C + v_D + v_E) \quad (1.1)$$

Therefore by applying a substitution, we get the following phase to neutral voltages equation

$$\begin{aligned}
V_a &= \frac{4}{5}V_A - \frac{1}{5}(V_A + V_B + V_C + V_D + V_E) \\
V_b &= \frac{4}{5}V_B - \frac{1}{5}(V_A + V_B + V_C + V_D + V_E) \\
V_c &= \frac{4}{5}V_C - \frac{1}{5}(V_A + V_B + V_C + V_D + V_E) \\
V_d &= \frac{4}{5}V_D - \frac{1}{5}(V_A + V_B + V_C + V_D + V_E) \\
V_e &= \frac{4}{5}V_E - \frac{1}{5}(V_A + V_B + V_C + V_D + V_E)
\end{aligned}$$

By using a power variant transformation in a stationary reference frame, the voltage V_{d-q} and V_{d3-q3} is obtained.

$$V_{d-q} = \frac{2}{5}V_{dc}(V_{an} + aV_{bn} + a^2V_{cn} + a^3V_{dn} + a^4V_{en}) \quad (1.2)$$

$$V_{d3-q3} = \frac{2}{5}V_{dc}(V_{an} + aV_{cn} + a^2V_{en} + a^3V_{bn} + a^4V_{dn}) \quad (1.3)$$

In (1.2) and (1.3) the $a=e^{j2\pi/5}$, $a^2=e^{j4\pi/5}$, $a^3=e^{-j4\pi/5}$ and $a^4=e^{-j2\pi}$. By applying (1.2) and (1.3) can be easily calculated the active vectors form in d-q and d3-q3 planes.

1.6 Space-Vector Decomposition for five phase machine

As was mentioned before, by applying more than three phases in terms of power rating, the greater possibility of freedom in design and reliability occur. One of the techniques for modelling a multi-phase machine is a Space-Vector Decomposition (VSD). The possibility of applying VSD exist for poly-phase machine which have a phase distribution 360/m electrical degrees. For this case, the n represents the number of phases. Space-Vector Decomposition can be also used with a half phase progression. In half phase progression is phase distribution of 180/m, this is usually used in split-phase machines [17], [18].

There are many possible arrangements of the stator, but in any of these cases, the VSD is a viable option, which can be used to modelling the electric machine.

1.6.1 Stator arrangements

For poly-phase machine stator windings, there are multiple design options. All option depends on the physical layout of phases in circumference. One of the most common options in a poly-phase machine is the asymmetrical layout, in which the phase progression is 360/m.

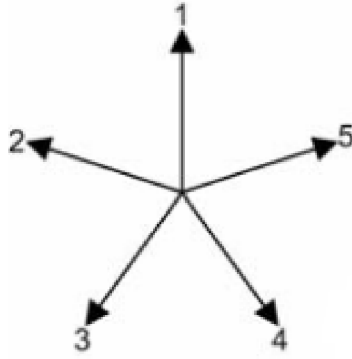


Figure 1.3: Symmetrical winding scheme for five phase (full progression).

When we take to a consideration case of a split-phase winding, which is created of x three-phase winding (sets) with x is considered as an even number. Then there is no possible way to reduce winding scheme to symmetrical N time three-phase with progression of $360/m$. On the other hand, it is possible to arrange such a winding into N time three-phase with $180/m$ progression[18].

As an example we can take $N=2$. In this arrangement of three-phase winding called as semi-12-phase or quasi-6-phase. It does not matter how we try to redistribute or redefined winding. There is no way to arrange winding to scheme with progression of $360/m$. Instead of using winding with the progression of $360/m$, we will use a winding with a progression of $180/m$. Such winding can be seen in Fig. 1.3 [17].

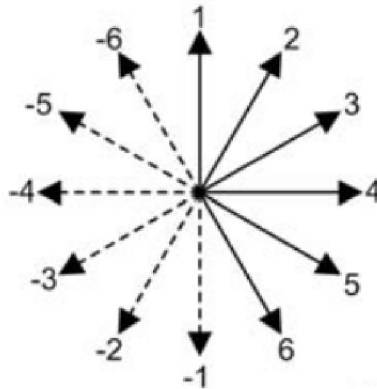


Figure 1.4: Dual three-phase winding (half phase progression).

1.6.2 VSD Full phase progression $360^\circ/m$

This section is focused on asymmetrical n -phase winding, with progression of $360/m$ electrical degree (full phase progression). One of the examples can be seen in Fig. 1.2.

Before we start the numerical calculation, we have to do a few modelling assumptions [17], [19]. Such as :

- Magnetic saturation effects are neglected
- Stator inductances are independent of rotor position
- Air-gap harmonics are not considered

As a first calculation, we start with inductance matrix L, which structure consist of $n \times n$. Progression of phase is in electrical radians α and mutual inductance L_k between phases shift by $k\alpha$ in electrical radians. This matrix is also referred to as symmetrical Toeplitz matrix structure (circulant matrix) [18].

$$L = \begin{bmatrix} L_0 & L_1 & L_2 & L_3 & L_4 \\ L_1 & L_0 & L_1 & L_2 & L_3 \\ L_2 & L_1 & L_0 & L_1 & L_2 \\ L_3 & L_2 & L_1 & L_0 & L_1 \\ L_4 & L_3 & L_2 & L_1 & L_0 \end{bmatrix} \quad (1.4)$$

If the matrix is circulant, it is possible to diagonalize the matrix by Fortescue transformation. In this case, the character "j" is representing an imaginary unit [17].

$$FLF^{-1} = \begin{bmatrix} \lambda_1 & 0 & 0 & 0 \\ 0 & \lambda_2 & 0 & 0 \\ 0 & 0 & \lambda_3 & 0 \\ 0 & 0 & 0 & \lambda_n \end{bmatrix} \quad (1.5)$$

$$[F]_{i,k} = \sqrt{\left(\frac{1}{n}\right)} \exp\left[j \frac{2\pi}{n} i(k-1)\right] \quad (1.6)$$

For i and k from (1.6) is used formula $\forall i, k = 1 \dots n$. Matrix (1.5) have some demerits such as that matrix is complex and non-orthonormal.

For real matrix F can occur two situation, one for odd and for even n. In both cases, the matrix is orthonormal and can transform the stator inductance matrix (1.4).

$$FLF^t = \begin{bmatrix} d_1 & 0 & 0 & 0 & 0 & 0 & 0 & 0 \\ 0 & d_1 & 0 & 0 & 0 & 0 & 0 & 0 \\ 0 & 0 & d_2 & 0 & 0 & 0 & 0 & 0 \\ 0 & 0 & 0 & d_2 & 0 & 0 & 0 & 0 \\ 0 & 0 & 0 & 0 & d_i & 0 & 0 & 0 \\ 0 & 0 & 0 & 0 & 0 & d_i & 0 & 0 \\ 0 & 0 & 0 & 0 & 0 & 0 & d_0 & 0 \\ 0 & 0 & 0 & 0 & 0 & 0 & 0 & d_{\frac{n}{2}} \end{bmatrix} \quad (1.7)$$

In case that structure of matrix (1.33) have an odd number of n, the last row is removed. Numerical evaluation can be seen in [17]

1.7 Testing of the five-phase machines

Over the years, many methods of testing aimed at poly-phase machines. These methods aimed at lowering the cost of testing, for example, mixed frequency testing (this method is also known as synthetic load) and back-to-back testing. Back-to-back testing is frequently used, for high-power machines. The requirement for this method are two identical machines, which are coupled to the same shaft. The machines have split functions, one of the machines operate as motor, while the second machine is operating as a generator. The procedure for loss measurement in back-to-back testing could be adapted for inverter-fed permanent magnet (PM) machines. As is mentioned earlier, two identical machines are mechanically coupled, but this time the single converter is parallel. As was mention, only one inverter is used, for that reason, the phase sequence of the generator has to be reversed. This reversed sequence is compared to the motoring phase sequence. Use of this combination of machines require a certain angle of the d-axes between the motor and the generator. This angel is used to get a circulating power. [20].

Back-to-back testing is a costly method, because it requires the coupling of the shafts of the machines and their power supplies. Also have to be considered a requirement of the space, because this method requires a substantial amount of space. For these reasons, alternative methods have been developed, such as synthetic load. Any kind of testing, which can be done on three-phase machines, can be adapted to poly-phase machines. However, it is easier to adopt the testing method, if the poly-phase machine has winding, which consists of x three-phase winding (x is meant as an integer). The best-case scenario is when the x is an even integer [20].

With time, other methods are considered to testing poly-phase machines, such us phantom loading, inverter-driven method and two frequency method. These methods are used, because they can provide the same temperature rise of testing machines, as in the case of testing the machine by a back-to-back method. However, in the case of the back-to-back method is possible to recirculate the power, if the dc links of converters are connected. In case of the other methods the recirculation of the power because of their losses [20].

In [20] new method is introduced, this method can test the machine without the need of mechanical coupling. The machine is tested with full-load and also is this method capable of circulating power through the different sectors, unlike phantom loading or two frequency methods. Method mentioned in [20] is based on that the two sections of the machine are connected. These sectors are opposite of each other and control (alternating) between generation and motoring mode.

2 Comparison of five-phase and three-phase machines

2.1 Slot pole number

This chapter is dealing with a comparison of three- and five-phase machines, as an example slot/pole combination. In Table 2.1, Table 2.3, Table 2.2 and Table 2.4 can be seen a calculations, which define the stability of winding in three- and five-phase machines. In the case of Tab.2.2 and Tab.2.4, if the value of calculation is not an integer, the winding is considered as unstable. In case of Slot/pole ratio, first we have to look at tables of stability after that the number decides which kind of winding it is (concentrated green, fractional-slot orange, integer-slot winding red, unbalance black). For example in Tab.2.1, the value in the third row, fourth column, is 0.67 for five-phase machine. This number also means that it is a stable concentrated winding.

Table 2.1: Number of slot per pole per phase five-phase.

		5 phase						
		Slot						
Pole		5	10	15	20	25	30	35
	2	0.50	1.00	1.50	2.00	2.50	3.00	3.50
	4	0.25	0.50	0.75	1.00	1.25	1.50	1.75
	6	0.17	0.33	0.50	0.67	0.83	1.00	1.17
	8	0.13	0.25	0.38	0.50	0.63	0.75	0.88
	10					0.50		
	12	0.08	0.17	0.25	0.33	0.42	0.50	0.58
	14	0.07	0.14	0.21	0.29	0.36	0.43	0.50
	16	0.06	0.13	0.19	0.25	0.31	0.38	0.44
18	0.06	0.11	0.17	0.22	0.28	0.33	0.39	

$$y_{rq} = \frac{S}{m \cdot p} \quad (2.1)$$

As it is mention above, the slot/pole/phase ration can be calculated, as a number of slots divided by the number of poles and phases. This number is also important in the calculation of winding factor. In the Tab.2.2 is calculated the stability of the winding by (2.1). The result is compared to an integer.

If the value is an integer then the winding is considered as stable. On the other hand, if the value is fractional the winding is considered as unstable, therefore is not desirable of any further calculations [21].

Table 2.2: Stable/unstable winding for five-phase.

		5 phase						
		Slot						
		5	10	15	20	25	30	35
Pole	2	1.00	2.00	3.00	4.00	5.00	6.00	7.00
	4	1.00	1.00	3.00	2.00	5.00	3.00	7.00
	6	1.00	2.00	1.00	4.00	5.00	2.00	7.00
	8	1.00	1.00	3.00	1.00	5.00	3.00	7.00
	10	0.20	0.40	0.60	0.80	1.00	1.20	1.40
	12	1.00	1.00	1.00	2.00	5.00	1.00	7.00
	14	1.00	2.00	3.00	4.00	5.00	6.00	1.00
	16	1.00	1.00	3.00	1.00	5.00	3.00	7.00
	18	1.00	2.00	1.00	4.00	5.00	2.00	7.00

$$k = \frac{S}{m \cdot GCD(S, p)} \quad (2.2)$$

In (2.2) is used a GCD. The GCD is the greatest common division between the number of slots S and the number of pole p . By calculating this number, it can be decided, if the winding is balanced or not. This case is similar as before. The evaluation is compared if it is an integer. If the value is an integer the winding is considered as a balance winding, otherwise, the winding is unbalanced. As an unbalance winding is considered that winding, which the combination of a number of poles and number of slots does not allow to arrange the coils in such a way that they produce a symmetrical system.

Table 2.3: Number of slot per pole per phase three-phase.

		3 phase						
		Slot						
		3	6	9	12	15	18	21
Pole	2	0.50	1.00	1.50	2.00	2.50	3.00	3.50
	4	0.25	0.50	0.75	1.00	1.25	1.50	1.75
	6			0.50			1.00	
	8	0.13	0.25	0.38	0.50	0.63	0.75	0.88
	10	0.10	0.20	0.30	0.40	0.50	0.60	0.70
	12			0.25			0.50	
	14	0.07	0.14	0.21	0.29	0.36	0.43	0.50
	16	0.06	0.13	0.19	0.25	0.31	0.38	0.44
	18							

Table 2.4: Stable/unstable winding for three-phase.

		3 phase						
		Slot						
		3	6	9	12	15	18	21
Pole	2	1.00	2.00	3.00	4.00	5.00	6.00	7.00
	4	1.00	1.00	3.00	2.00	5.00	3.00	7.00
	6	0.33	0.67	1.00	1.33	1.67	2.00	2.33
	8	1.00	1.00	3.00	1.00	5.00	3.00	7.00
	10	1.00	2.00	3.00	4.00	1.00	6.00	7.00
	12	0.33	0.33	1.00	0.67	1.67	1.00	2.33
	14	1.00	2.00	3.00	4.00	5.00	6.00	1.00
	16	1.00	1.00	3.00	1.00	5.00	3.00	7.00
	18	0.33	0.67	0.33	1.33	1.67	0.67	2.33

As can be seen from the tables above, the three-phase machine has more unstable winding compared to five-phase winding. As a next step, the winding factor can be calculated. As is mention in [22], the total winding factor consists of pitch factor k_p and the distribution factor k_d . Distribution factor is calculated by equation (2.3). The equations for the distribution factor from [22], are calculated based on the geometric sum of voltage phasors.

$$k_d = \frac{\sin(\frac{v \cdot q \cdot \alpha_u}{2})}{q \cdot \sin(\frac{v \cdot \alpha_u}{2})} \quad (2.3)$$

In equation (2.3) the v means the number of harmonic, α_u is a slot angel and q is a number of slots per pole pair per phase. The slot angle can be estimated by equation 2.4.

$$\alpha_u = \frac{2p\pi}{S} \quad (2.4)$$

It is possible to adjust the equation (2.3) for the three-phase machine, in which the calculation is shortened. So the equation (2.5) is for instance of m equal to three, for the first harmonic.

$$k_d = \frac{1}{2q \sin(\frac{\pi}{6q})} \quad (2.5)$$

Now the attention will be focus on the pitch factor. In case that the ends of coils are not at distance 180 electrical degree and it is a short-pitched winding, the pitched factor is not equal one and therefore the winding factor is going to be lowered by the value of pitch factor calculated by equation (2.6).

$$k_p = \sin(v \frac{y}{y_Q} \frac{\pi}{2}) \quad (2.6)$$

In this equation the y is pitch and y_Q is the pole pitch. If a pitch is equal to pole the pitch factor is equal one $k_p = 1$, otherwise the pitch is less than pole pitch and $k_p < 1$.

2.2 Performance comparison of poly-phase induction machines

In this part, the performance of five and three-phase machines will be compared. Both machines were designed with the same dimensions and ratings in paper [23]. But the number of the slot in stator and rotor had to be changed to fit the five-phase winding. These numbers were chosen to achieve a similar ratio between stator and rotor slot number. The rating and dimensions can be seen in Tab. 2.1 [23].

Table 2.5: Rating and dimensions of machines [23]

data	three-phase	five-phase
power (kW)	5.5	5.5
phase voltage (V)	220	220
frequency (f)	60	60
number of pole pairs (p)	2	2
external stator diameter (mm)	182	182
internal stator diameter (mm)	115	115
axial length (mm)	140	140
airgap length (mm)	0.6	0.6
winding pitch (slots)	9	12
number of stator slots	36	60
number of rotor slots	28	44

As was mentioned above, the differences in stator and rotor slots for three and five-phase machines cause a difference in volume of conductor material. In this case, the five-phase machine has a fewer conductor material in stator and rotor. To be exact the stator winding of the five-phase machine is about 82 % of the volume in the three-phase machine. And in case of the rotor, the winding of five-phase is 89 % of volume in the three-phase machine.

The comparison is under steady-state model. Both machines are under sinusoidal stator voltage and in case of the five-phase machine, the third harmonic current component is present.

In Tab. 2.5 are shown the output values of the machines. The five-phase machine is divided into three parts. As can be seen in Table 2.5 the second column is for the three-phase machine, which is fed by sinusoidal voltage with any third harmonic (the machines is in star connection). Although because of the saturation, the third harmonic magnetic flux density appears in the air-gap, so it induces harmonic in the rotor (voltages

and currents). This could be used to produce an additional useful torque. For this case, the value of the magnetic flux density is slightly higher than the fundamental magnetic flux density (around 3.8 % higher). This fact results in the generation of additional torque (the value is around 0.14 %). For additional torque component to be compelling value only if the machine is heavily saturated.

Table 2.6: Performance comparison of the three and five phase machines [23].

data	three-phase	five-phase (a)	five-phase (b)	five-phase (c)
P_0 [W]	5500	5500	5500	5500
V_1 [V]	220	220	220	220
B_M [T]	0.707	0.766	0.671	0.700
P_{sj} [W]	320.7	324.0	357.1	298.6
P_{rj} [W]	150	148.7	145.6	158.9
P_{mag} [W]	130	156.8	167.5	139.2
P_{mech} [W]	37	37	37	36.8
s [%]	2.58	2.54	2.49	2.72
T [Nm]	29.95	29.94	29.92	29.99
η [%]	89.7	89.2	88.6	89.7
$\cos(\phi)$ [-]	0.805	0.788	0.810	0.847
B_3/B_1 [%]	3.8	1.5	14	6
T_3/T_1 [%]	0.14	0.20	1.79	0.38

(In case of five-phase a is fed by sinusoidal voltage without third harmonics, five-phase b and c are with third harmonics. For five-phase machine b, the third harmonic voltage is modified to produce a trapezoidal shape. At the same time the five-phase machine c third harmonic was adjusted to achieve a maximal efficiency.)

In the third column of Table 2.6 (five-phase a), the results of the five-phase machine is shown. This machine is fed just by sinusoidal voltage (same as three-phase machine). As the first comparison, we could take a peak of magnetic flux density in air-gap. The value for the five-phase machine is 0.766 T, which it is around 8 % higher than, in case of three-phase machine 0.707 T. In case of the same peak of magnetic flux density B_M is needed, the stator voltage for the five-phase machine should be lowered. The saturation is slightly higher than the fundamental (around 1.5 % higher). Also, the joule losses in stator and rotor and mechanical losses are almost the same. On the other hand, if we look at the magnetic losses significantly higher (20 % higher than three-phase). This fact results in lower efficiency (the difference is 0.5 %). For this case, the five-phase machine does not generate any advantages in efficiency or power factor [23].

In the fourth column of Table 2.6, are results of the five-phase machine b. This machine is operating with trapezoidal induction in the air-gap. In this case, the third har-

monic is higher than the fundamental about 14 %. For this machine, the magnetic losses are the highest 167.5 W. And therefore, the efficiency is the worst of all compared machines 88.6 %. The decline of the efficiency is not caused only by magnetic losses, but also that the Joule losses are increased. The increase of the stator losses is caused by the increase of third harmonic current, and the magnetic losses comes from the increase of eddy current losses. The increase in produce torque is around 1.79 %, if the fundamental torque is considered as a base value [23].

As a fifth and last column of Table 2.2, are results of the five-phase machine c. This machine is adjusted to achieve maximal efficiency. This adjustment was done on the winding (the pitch has been shortened by only one slot). This shortening results in decreasing the third harmonic component to 6 %. This machine has a similar overall losses as a three-phase machine, which results in the same efficiency 89.7 %.

If it is taken to a consideration the Tables 2.5 and 2.6, it can be seen that the five-phase machines have similar performance as the three-phase machines. But they have a lower volume of conductor material, which results in lower production cost and their higher reliability [23].

3 Analytical methods of the five-phase machines

3.1 Mathematical model of the Five Phase PM motor

This part will focus on the mathematical model of the five-phase motor. This model contains parameters such as torque, voltage and voltage equations. These parameters are established for the rotating frame.

As a first parameter will be voltage. The equations for stator voltage are given[24] and [9]:

$$V_S = R_S I_S + \frac{d\Psi_S}{dt} \quad (3.1)$$

where R_S is stator resistance, I_S is stator current and Ψ_S is stator flux linkage.

If a substitution is applied on stator flux linkage windings with considering the currents in the stator winding such as stator currents and stator winding inductances. The equation is [25]:

$$\Psi_S = L_{SS} I_S + \Psi_m \quad (3.2)$$

In this case, the Ψ_m represent a matrix of flux linkage caused by PM and L_{SS} represents a stator inductance matrix which includes self and mutual inductances of the stator. Stator current is a matrix of currents in stator phases[25]. It is given by:

$$I_S = \begin{bmatrix} I_{as} & I_{bs} & I_{cs} & I_{ds} & I_{es} \end{bmatrix}^t \quad (3.3)$$

Stator inductance matrix is a symmetric 5 by 5 matrix of self inductances of every phase. The form of the matrix is [25]:

$$L_{SS} = \begin{bmatrix} L_{aa} & L_{ab} & L_{ac} & L_{ad} & L_{ae} \\ L_{ab} & L_{bb} & L_{bc} & L_{bd} & L_{be} \\ L_{ac} & L_{bc} & L_{cc} & L_{cd} & L_{ce} \\ L_{ad} & L_{bd} & L_{cd} & L_{dd} & L_{de} \\ L_{ae} & L_{be} & L_{ce} & L_{de} & L_{ee} \end{bmatrix} \quad (3.4)$$

In equation 1.4 the elements in diagonal are self-inductance of each phase and the off-diagonal are the mutual inductances between each phases pair.

In this case, will be considered only the fundamental and third harmonics component. Only the fundamental and third harmonics are considered due to simplifying the

model. Due to this fact, the Ψ_m can be written as [25]:

$$\Psi_m = \Psi_{m1} \begin{bmatrix} \sin(\theta_r) \\ \sin(\theta_r - \frac{2\pi}{5}) \\ \sin(\theta_r - \frac{4\pi}{5}) \\ \sin(\theta_r + \frac{4\pi}{5}) \\ \sin(\theta_r + \frac{2\pi}{5}) \end{bmatrix} + \Psi_{m3} \begin{bmatrix} \sin(3\theta_r) \\ \sin 3(\theta_r - \frac{2\pi}{5}) \\ \sin 3(\theta_r - \frac{4\pi}{5}) \\ \sin 3(\theta_r + \frac{4\pi}{5}) \\ \sin 3(\theta_r + \frac{2\pi}{5}) \end{bmatrix} \quad (3.5)$$

As is mentioned above the Ψ_{m1} and Ψ_{m3} are amplitudes of the first and third harmonics and θ_r is a rotor position.

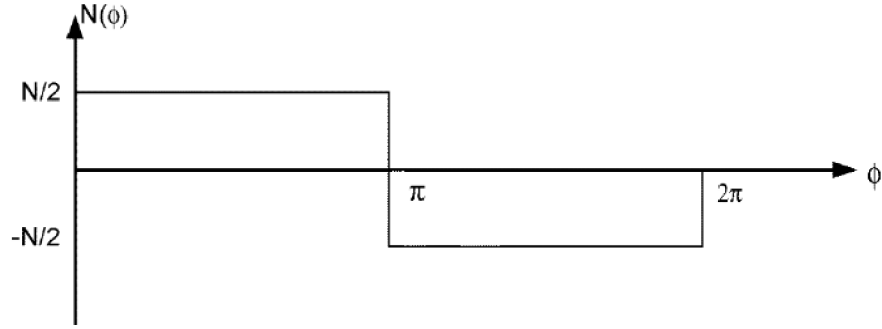


Figure 3.1: Stator winding [25].

The axis of one phase is used to determine the circumferential angle ϕ . The circumferential angle is used to define the winding function in Fig. 1.1.

$$\begin{aligned} N_a(\phi) &= \frac{4}{\pi} \frac{N_s}{p} \left[\cos \phi - \frac{1}{3} \cos 3\phi \right] \\ N_b(\phi) &= \frac{4}{\pi} \frac{N_s}{p} \left[\cos\left(\phi - \frac{2\pi}{5}\right) - \frac{1}{3} \cos 3\left(\phi - \frac{2\pi}{5}\right) \right] \\ N_c(\phi) &= \frac{4}{\pi} \frac{N_s}{p} \left[\cos\left(\phi - \frac{4\pi}{5}\right) - \frac{1}{3} \cos 3\left(\phi - \frac{4\pi}{5}\right) \right] \\ N_d(\phi) &= \frac{4}{\pi} \frac{N_s}{p} \left[\cos\left(\phi + \frac{2\pi}{5}\right) - \frac{1}{3} \cos 3\left(\phi + \frac{2\pi}{5}\right) \right] \\ N_e(\phi) &= \frac{4}{\pi} \frac{N_s}{p} \left[\cos\left(\phi + \frac{4\pi}{5}\right) - \frac{1}{3} \cos 3\left(\phi + \frac{4\pi}{5}\right) \right] \end{aligned}$$

In this case, the motor has concentrated winding. At the same time, air-gap is uniform and the inductances of the stator (self and mutual) constant values. As it was mentioned before, there are considered only the first and third harmonics component. The winding function for each phase can be seen in the equation above. In this equation

N_s represents the number of turns, p represents the number of pole and ϕ is a spatial angel.

Now the focus will shift on the self and mutual inductances of the stator. These inductances can be calculated by the right winding function, which corresponds to the stator phase inductances [25].

$$L_{aa} = L_{bb} = L_{cc} = L_{dd} = L_{ee} \quad (3.6)$$

$$L_{aa} = \frac{\mu_0 r l}{g} \pi N_{s1}^2 + \frac{\mu_0 r l}{g} \pi N_{s3}^2 \quad (3.7)$$

$$L_{ab} = L_{bc} = L_{cd} = L_{de} = L_{ae} \quad (3.8)$$

$$L_{ab} = \cos \frac{2\pi}{5} L_{ms1} + \cos 3 \frac{2\pi}{5} L_{ms3} \quad (3.9)$$

$$L_{ac} = L_{bd} = L_{ce} = L_{da} = L_{ce} \quad (3.10)$$

$$L_{ac} = \cos \frac{4\pi}{5} L_{ms1} + \cos 3 \frac{4\pi}{5} L_{ms3} \quad (3.11)$$

As a next step are values of N_{s1} and N_{s2} calculated by (3.12) and (3.13)

$$N_{s1} = \frac{4 N_s}{\pi P} \quad (3.12)$$

$$N_{s2} = -\frac{1}{3} \frac{4 N_s}{\pi P} \quad (3.13)$$

To reduce the complexity of the machine model, a coordinate transformation have to be introduced. This will be an arbitrary coordinate transformation. This transformation transfers the parameters of the poly-phase machine into a reference frame. The reference frame is a rotating frame with an angular velocity. The transformation is applied also to third harmonic. This is due to including the effect of the third harmonic d_1 , q_1 , d_3 and q_3 . The d and q axis are rotating at different speeds for the first and third harmonics. For the first harmonic the d_1 and q_1 are rotating at synchronous speed [25]. The d_3 and q_3 are rotating at velocity three times greater than synchronous speed.

As a transformation matrix is used (3.14)

$$T(\theta_r) = \frac{2}{5} \begin{bmatrix} \sin\theta_r & \sin(\theta_r - \frac{2\pi}{5}) & \sin(\theta_r - \frac{4\pi}{5}) & \sin(\theta_r + \frac{4\pi}{5}) & \sin(\theta_r + \frac{2\pi}{5}) \\ \cos\theta_r & \cos(\theta_r - \frac{2\pi}{5}) & \cos(\theta_r - \frac{4\pi}{5}) & \cos(\theta_r + \frac{4\pi}{5}) & \cos(\theta_r + \frac{2\pi}{5}) \\ \sin 3\theta_r & \sin 3(\theta_r - \frac{2\pi}{5}) & \sin 3(\theta_r - \frac{4\pi}{5}) & \sin 3(\theta_r + \frac{4\pi}{5}) & \sin 3(\theta_r + \frac{2\pi}{5}) \\ \cos 3\theta_r & \cos 3(\theta_r - \frac{2\pi}{5}) & \cos 3(\theta_r - \frac{4\pi}{5}) & \cos 3(\theta_r + \frac{4\pi}{5}) & \cos 3(\theta_r + \frac{2\pi}{5}) \\ \frac{1}{\sqrt{(2)}} & \frac{1}{\sqrt{(2)}} & \frac{1}{\sqrt{(2)}} & \frac{1}{\sqrt{(2)}} & \frac{1}{\sqrt{(2)}} \end{bmatrix} \quad (3.14)$$

As first the transformation is used on stator voltage. So the equation for stator voltage is as follows

$$V_{ds1} = r_s i_{ds1} - \omega \Psi_{qs1} + \frac{d\Psi_{ds1}}{dt} \quad (3.15)$$

$$V_{qs1} = r_s i_{qs1} + \omega \Psi_{ds1} + \frac{d\Psi_{qs1}}{dt} \quad (3.16)$$

$$V_{ds3} = r_s i_{ds3} - \omega \Psi_{qs3} + \frac{d\Psi_{ds3}}{dt} \quad (3.17)$$

$$V_{qs3} = r_s i_{qs3} + \omega \Psi_{ds3} + \frac{d\Psi_{qs3}}{dt} \quad (3.18)$$

When the voltages are transformed, the stator flux linkage is next. Stator flux linkage after transformation is given by:

$$\Psi_{ds1} = (L_{ls} + \frac{5}{2}L_{ms1})i_{ds1} + \Psi_{m1} \quad (3.19)$$

$$\Psi_{qs1} = (L_{ls} + \frac{5}{2}L_{ms1})i_{qs1} \quad (3.20)$$

$$\Psi_{ds3} = (L_{ls} + \frac{5}{2}L_{ms3})i_{ds3} + \Psi_{m3} \quad (3.21)$$

$$\Psi_{qs3} = (L_{ls} + \frac{5}{2}L_{ms3})i_{qs3} \quad (3.22)$$

After the calculation of stator flux linkages, we can calculate the electromagnetic torque. The electromagnetic torque is equal to partial derived co-energy W_{co} concerning mechanical rotor angel θ_{rm} .

$$T = \frac{\partial W_{co}}{\partial \theta_{rm}} \quad (3.23)$$

The co-energy is give by

$$W_{co} = \frac{1}{2} I_s^T L_S I_S + I_s^T \Psi_m \quad (3.24)$$

By using partial derivative of co-energy with respect to mechanical rotor angel, will obtain an equation for electromagnetic torque

$$T = I_s^T \frac{P}{2} \frac{\partial \Psi_m}{\partial \theta_r} \quad (3.25)$$

Equation (1.25) can be overwritten, than the equation is

$$T = \left(\frac{1}{T(\theta_r)} i_{d1q1d3q3s} \right)^t \frac{P}{2} \frac{\partial \Psi_m}{\partial \theta_r} \quad (3.26)$$

For the next step has to be applied a pseudo-orthogonal property of transformation matrix. The pseudo-orthogonal property

$$\frac{1}{T(\theta_r)} = \frac{5}{2} T^t(\theta_r) \quad (3.27)$$

If (3.27) is applied into (3.26) the electromagnetic torque can be written such as [25]:

$$T = \frac{5P}{4} (\Psi_{m1} i_{qs1} + 3\Psi_{m3} i_{qs3}) \quad (3.28)$$

Now for the final step in expression of electromagnetic torque is by applying substitution from (3.19) and (3.21) into (3.28). After adjusting the equation electromagnetic torque is give by[25]:

$$T = \frac{5P}{4} (\Psi_{ds1} i_{qs1} - \Psi_{qs1} i_{ds1} + 3\Psi_{ds3} i_{qs3} - 3\Psi_{qs3} i_{ds3}) \quad (3.29)$$

In (3.29) the Ψ_{ds1} , Ψ_{qs1} , Ψ_{ds3} , Ψ_{qs3} represents the stator fluxes in d_1 , q_1 , d_3 and q_3 axes. The i_{qs1} , i_{ds1} , i_{qs3} and i_{ds3} represent the stator currents in d_1 , q_1 , d_3 and q_3 axes. These currents are transformed. As can be seen from (3.29) by keeping the third harmonic, the torque has been improved[25].

3.2 Short-circuit of five-phase machine

At the start of the chapter will be about a one phase short circuit. The shift of the phases is $2\pi/5$. The phases name will be changed to A, B, C, D and E.

3.2.1 Short-circuit of one phase

Imagine that phase C is short-circuited, the equation of the voltage in the short-circuit phase can be seen in (3.30). This equation is given according to Lentz's law[26].

$$V_C = 0 = R_C I_C + \frac{L_C dI_C}{dt} + M_1 \left(\frac{dI_A}{dt} + \frac{dI_E}{dt} \right) + M_2 \left(\frac{dI_B}{dt} + \frac{dI_D}{dt} \right) + \frac{d\Phi_{C0}}{dt} \quad (3.30)$$

The Φ_{C0} is a non-load flux for phase C, R_C represent resistance of phase C, L_C phase inductance, M_1 represent mutual inductance between phase and not a consecutive phase, M_2 represent similarly as M_1 mutual inductance but it is different in that the inductance between phase and consecutive phase[26].

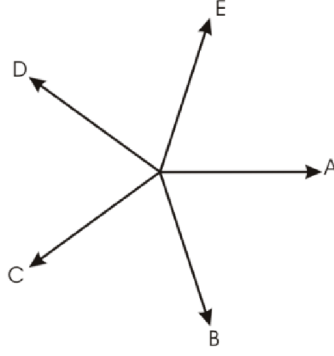


Figure 3.2: Shift between phases [26].

3.2.2 Short-circuit of two phases

In case of short-circuit of two phases, two option can occur. One, if the phases are consecutive (As an example B and C). The second option is, if the phases are non- consecutive(phases C and E).

As is mentioned above, the first case the short-circuit is on phases B and C. Values of voltage for phases B and C can be calculated similarly to one phase circuit (3.30)[26].

$$V_C = 0 = R_C I_C + \frac{L_C dI_C}{dt} + M_1 \left(\frac{dI_A}{dt} + \frac{dI_E}{dt} \right) + M_2 \left(\frac{dI_B}{dt} + \frac{dI_D}{dt} \right) + \frac{d\Phi_{C0}}{dt} \quad (3.31)$$

$$V_B = 0 = R_B I_B + \frac{L_B dI_B}{dt} + M_1 \left(\frac{dI_D}{dt} + \frac{dI_E}{dt} \right) + M_2 \left(\frac{dI_A}{dt} + \frac{dI_C}{dt} \right) + \frac{d\Phi_{B0}}{dt} \quad (3.32)$$

By equation (3.31) and (3.32) can be express the short-circuit currents. For the second option, the short-circuit occur on phases C and E. Likewise in the first option, similar expressions for phases C and E is acquired[26].

$$V_C = 0 = R_C I_C + \frac{L_C dI_C}{dt} + M_1 \left(\frac{dI_A}{dt} + \frac{dI_E}{dt} \right) + M_2 \left(\frac{dI_B}{dt} + \frac{dI_D}{dt} \right) + \frac{d\Phi_{C0}}{dt} \quad (3.33)$$

$$V_B = 0 = R_E I_E + \frac{L_c dI_E}{dt} + M_1 \left(\frac{dI_B}{dt} + \frac{dI_C}{dt} \right) + M_2 \left(\frac{dI_A}{dt} + \frac{dI_D}{dt} \right) + \frac{d\Phi_{B0}}{dt} \quad (3.34)$$

When the short-circuit currents are calculated, new currents values have to be resolved for healthy phases (phases A, B and D). This could be done by the optimization algorithm. Same goes for case of non-consecutive phases[26].

3.3 Open-circuit of five phase machine

As was mentioned before, one of the advantages of polyphase machines is the fault tolerance. This time in case of open-circuited. As is mentioned in [27], the open-circuited

is one of the common faults found in poly-phase machines. When the fault occurs the currents of the healthy phase (phase with currents with any problems) has to be changed, for the fact that one or more phases can not be supplied by the currents.

The strategies for modification of currents may be, genetic algorithm (GA), On-line optimal current (OC), Lagrange multipliers (LM). More information to each method can be found in [27], [2], [28] and [3]. This thesis focus will be on LM, but in chapters (3.3.2) and (3.3.3) are shown a method of GA and OC.

3.3.1 Lagrange multipliers

At the start of Lagrange multipliers, we need to define a function, which has to be minimized. This function will be represented by minimizing the copper losses (3.35).

$$P_{cu} = R\mathbf{i}^T\mathbf{i} \quad (3.35)$$

Where \mathbf{i} represents vector of currents.

$$\mathbf{i} = \begin{bmatrix} i_1 \\ i_2 \\ \dots \\ \dots \\ i_n \end{bmatrix} \quad (3.36)$$

In this case, n represents the number of phases. As a next step, the constraints for the main function are defined:

- The output power should be equal to the required power.
- The sum of currents in healthy phases should be equal to zero.

$$P_w = P_{out} \quad (3.37)$$

$$\sum_{j=1}^n i_j = \mathbf{H}\mathbf{i} = 0 \quad (3.38)$$

Where \mathbf{H} represents the vector of ones, P_w represents the required power (wanted power) and P_{out} represents the output power.

$$P_{out} = \mathbf{V}^T\mathbf{i} \quad (3.39)$$

After the constrains are defined, the main equation can be written

$$f = R\mathbf{i}^T\mathbf{i} + \lambda_1(\mathbf{V}^T\mathbf{i} - P_w) + \lambda_2(\mathbf{H}\mathbf{i}) \quad (3.40)$$

Main function can be seen at (3.40). λ_1 and λ_2 represents the Lagrange multipliers. This function will be partial derivative with respect to the j th current.

$$\frac{\partial f}{\partial i_j} = 0 = 2Ri_j + \lambda_1(V_j) + \lambda_2 \quad (3.41)$$

The derivation is set to zero to be optimized. As next step is a substitution from (3.41) into (3.39), which yields:

$$P_w = \sum_{j=1}^n V_j \left(-\frac{\lambda_1(V_j)}{2R} - \frac{\lambda_2}{2R} \right) = -\lambda_1 \frac{(\mathbf{V}^T \mathbf{V})}{2R} - \lambda_2 \frac{\mathbf{V}^T}{2R} \quad (3.42)$$

In (3.42) is define the new wanted power with LM. Also the substitution from (3.41) into (3.38) yields:

$$-\lambda_1 \frac{(\mathbf{H}\mathbf{V})}{2R} - \lambda_2 \frac{n}{2R} = 0 \quad (3.43)$$

Now when we have two-equation, the LM can be calculated from (3.42) and (3.43).

$$\lambda_1 = 2R \frac{\mathbf{V}P_w}{-n\mathbf{V}^T\mathbf{V} + (\mathbf{H}\mathbf{V})^2} \quad (3.44)$$

$$\lambda_2 = 2R \frac{P_w \mathbf{H}\mathbf{V}}{-n\mathbf{V}^T\mathbf{V} + (\mathbf{H}\mathbf{V})^2} \quad (3.45)$$

By applying (3.44) and (3.45) into (3.41), the current is given as :

$$\mathbf{i} = P_w \frac{n\mathbf{V} - \mathbf{H}^T\mathbf{H}\mathbf{V}}{n\mathbf{V}^T\mathbf{V} - (\mathbf{H}\mathbf{V})^2} \quad (3.46)$$

Now the equation for the current is express, so the calculation for each state of the five-phase machine can be done.

Above mention calculation are considered for star connection of the machine. If the connection would change to pentagonal or pentacle the vector H would have to change accordingly to the situation. More information to each situation of connection can be found in [3] and [29]. Each of the connection with the direction of the currents can be seen in Figure 3.3.

3.3.2 Calculation of currents

As for the first calculation, the normal state of the machine is considered. The value of the torque wanted is 10 Nm. This value was calculated for two scenarios with back EMF amplitude of 100 V.

As can be seen in Figure 3.4, the amplitude of each phase is five amperes. This current has been calculated with ideal sinusoidal back-emf, but if the curves of back-emf are not

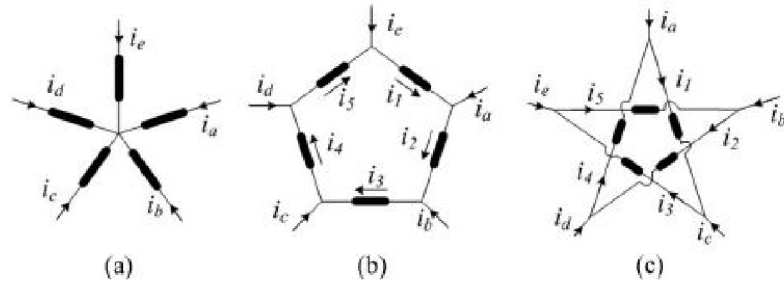


Figure 3.3: Configuration of the windings. a) star, b) pentagon, c) pentacle.

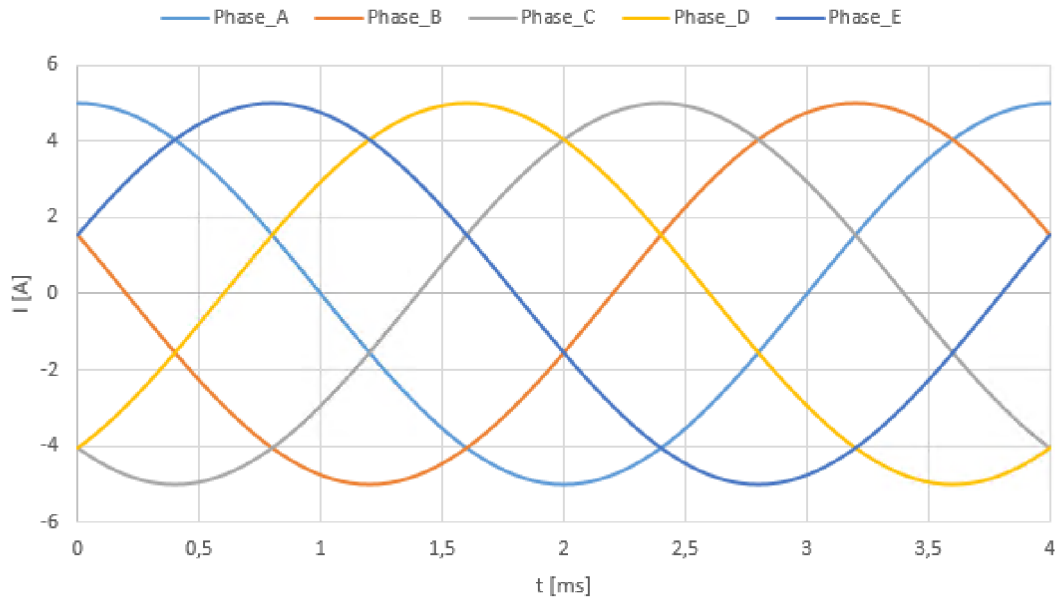


Figure 3.4: All healthy phases (sinusoidal back EMF).

perfectly sinusoidal can be just replaced. The amplitude of the current is 5.5 A in each phase. The curves of currents can be seen in Figure 3.5.

For the next step, currents in one open phase situation are evaluated (phase A is considered as an open phase). As can be seen from Figure (3.6) the currents have lost their sinusoidal curves. The amplitudes for all phase differ. For the phases B and E, the amplitude of the current is 8.75 A and currents in phase C and D are 7.1 A.

The amplitude of phase B is 1.59 times higher than in a normal phase operation. For the phase C, this value is 1.29. The multiplier of amplitude for phase B and E is quite high, but it is necessary to say those values are to achieve a full torque as in the healthy case (10 N.m of torque). If the value of torque (it can also use power) is lowered to 80% (8 N.m of torque) the multiplier of amplitudes are lowered to 1.27 and 1.02 respectively. These curves of currents for torque which is lowered to 8 N.m can be seen in Figure (3.7).

Now let us have a look at cases in which are 2 phases open. Similarly, as in short circuit, there are two ways which the calculations can go. Those are if phases are con-

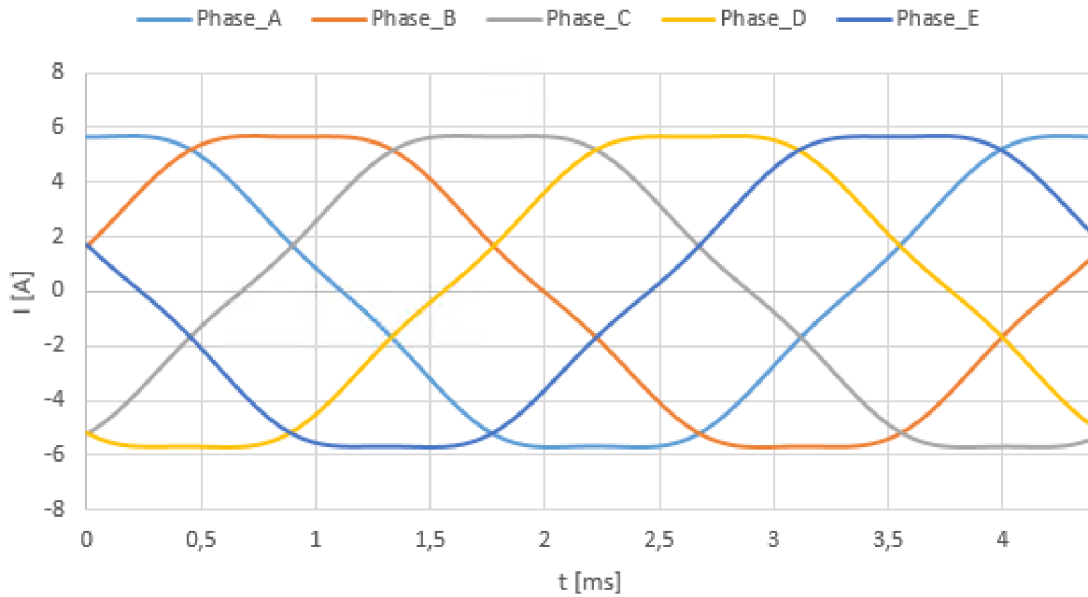


Figure 3.5: All healthy phases (non sinusoidal back EMF).

secutive or phases are non-consecutive. As the first one will be when 2 phases are open they are consecutive (phases A and B are open). If the wanted torque is nominal, then the amplitudes for phases of C and E are 16.4 A which is quite high from the normal amplitude of currents in healthy case. This amplitude is almost 3 times higher. As for the phase D the amplitude went from 5.5 A to 21.4 A. Which is 3.9 times higher than normal operation. This can be seen from Figure (3.8).

In case that the torque is lowered to previously 8 N.m, the amplitudes of phases C and E decrease to the value of 13.1 A. This amplitude is almost 2.4 times higher from normal operation, for phase C 1.85 and for phase E 1.5 times higher from operation under operation with one phase open. For the phase D, the amplitude has been lowered to 17.1 A. This value of amplitude is 3.1 times higher than normal operation and 2.4 times higher than operation with one phase open. This case can be seen in Figure 3.9.

As a last case which was calculated for consecutive open phase scenario, was the case when the torque is decreased to 60% on nominal torque (value of torque 6 N.m). In this scenario, the amplitude of C and E phase is 9.8 A. For phase D the maximum value of current is 12.8 A. These values are significantly lower than in case of need the full (nominal) torque. In short, they are 1.67 times lower for all phases. The values of currents are still quite high and would create significant copper losses. But if the capability of the machine allowed for higher currents in phase. It is possible to get the nominal torque with just three phases.

If the phases are non-consecutive as an example phase A and C. The amplitudes of each healthy phases differ from the case when the 2 phases are consecutive. As a first part, the calculation is for nominal torque. For phases D and E, the amplitudes are 12.7

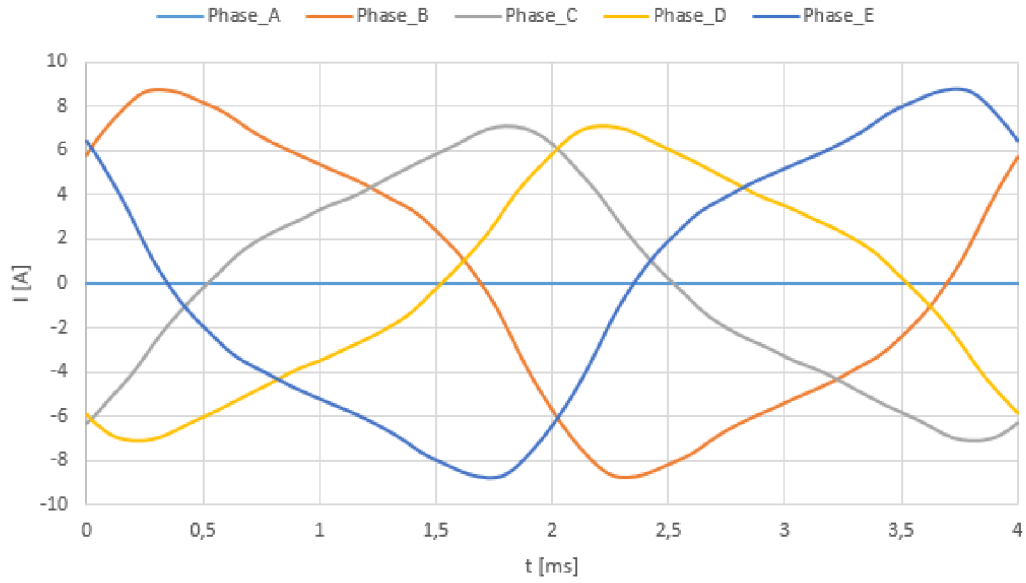


Figure 3.6: Reconfiguration one phase open (Phase A is open, 10 Nm).

A and for phase B 8.4 A. As can be seen this difference is for phase E 3.7 A, for phase D is 8.7 A. When we continue to the 8 N.m of torque. The amplitudes are 10.1 A for D and E, and 6.8 A for phase B. The amplitudes in phases D and E are still quite high, 1.84 times higher than normal. But when we get to the 60% nominal torque, the multiplier of amplitudes get us to the reasonable area. At the start the phase B the amplitude is 5.1 A, and for phases D and E is 7.6 A. The curves of currents for 6 Nm of torque can be seen if Figure 3.10.

3.3.3 Different method of calculation currents Genetic Algorithm

In this chapter are considered a different approach to the problem of reconfiguration of currents. One of the possible approaches is the Genetic Algorithm. In the case of a GA, there are many possible ways to define the calculation. The reason for many possible way is that it depends on you how many independent variables you create. As an example in the case of one phase open circuit, you can choose that you do not want to change the amplitudes of current and just change the phase shift of each phase. Also, it has to be considered how many independent variables is used because with the increase of variables the time of calculation is also growing. For this thesis will be based on articles [30], [31] and [32]. In [30] there are 2 options calculated for five-phase machines. Those are currents reconfiguration with 6 and 12 parameters. Both cases are based on these equations:

$$I_A = I_{max} \cos(\omega t + \varphi) \quad (3.47)$$

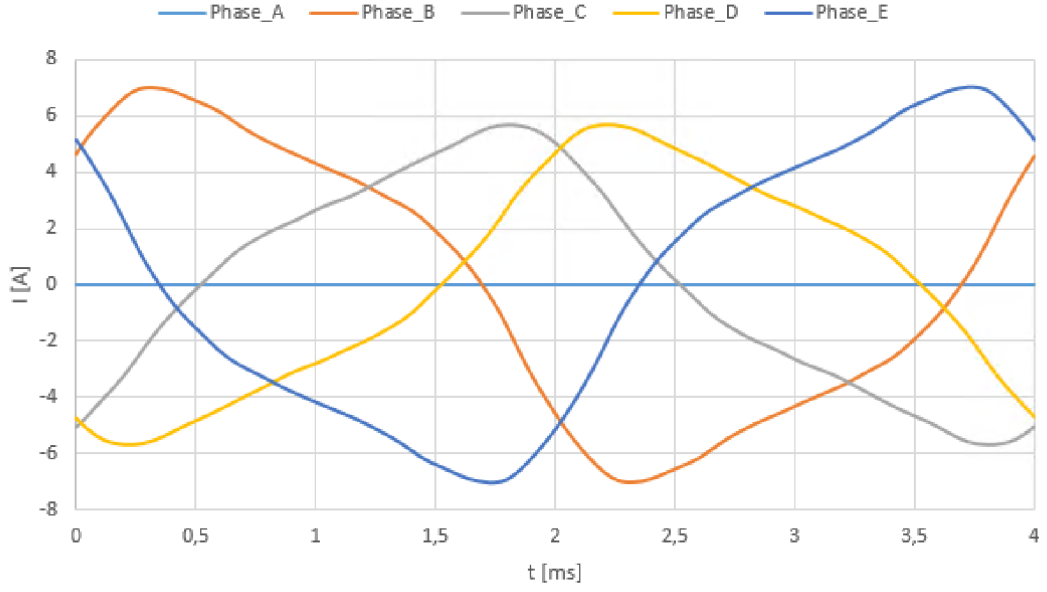


Figure 3.7: Reconfiguration one phase open (Phase A is open, 8 Nm).

$$I_B = I_{max} \cos(\omega t + \varphi - 2\frac{\pi}{5}) \quad (3.48)$$

$$I_C = 0 \quad (3.49)$$

$$I_D = I_{max} \cos(\omega t + \varphi - 6\frac{\pi}{5}) \quad (3.50)$$

$$I_E = I_{max} \cos(\omega t + \varphi - 8\frac{\pi}{5}) \quad (3.51)$$

In the case of current reconfiguration with six independent variables, there are 3 variables which are used to define the amplitudes (m_1, m_2, m_3) of currents, and 3 are used for phase shift ($\beta_1, \beta_2, \beta_3$). With this knowledge the equation (3.74-3.51) change to:

$$I_A = I_{max} \cos(\omega t + \varphi) \quad (3.52)$$

$$I_B = m_1 I_{max} \cos(\omega t + \varphi - 2\frac{\pi}{5} - \beta_1) \quad (3.53)$$

$$I_C = 0 \quad (3.54)$$

$$I_D = m_2 I_{max} \cos(\omega t + \varphi - 6\frac{\pi}{5} - \beta_2) \quad (3.55)$$

$$I_E = m_3 I_{max} \cos(\omega t + \varphi - 8\frac{\pi}{5} - \beta_3) \quad (3.56)$$

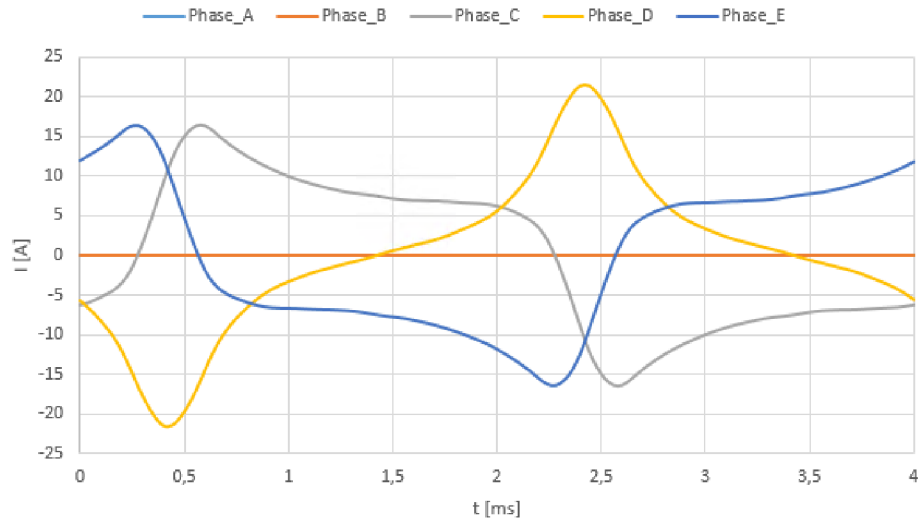


Figure 3.8: Reconfiguration two phases open (Phases A and B are open, 10 Nm).

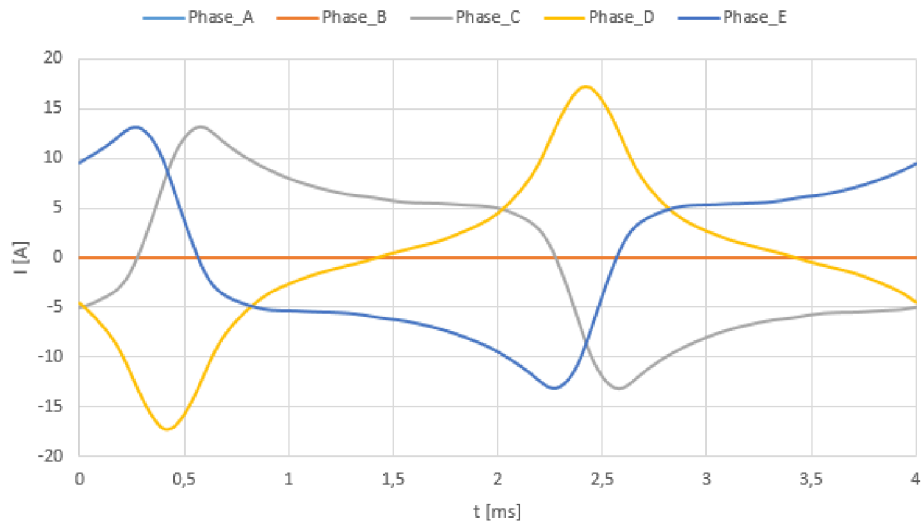


Figure 3.9: Reconfiguration two phases open (Phases A and B are open, 8 Nm).

It is needed to say that in this GA calculation with 100 individuals in a generation. And in total there are 500 generations. Also the condition which was to reduce the torque ripple and residual currents. For this condition, constraints need to be set and those keep a mean torque weakened by 10% to the nominal torque and copper losses can not be higher than 20%.

Table 3.1: Values of parameter using GA optimization(six parameters) [30].

m_1	m_2	m_3	β_1	β_2	β_3
1.333	1.292	1.247	0.489	-0.484	0.328

The curves of currents can be seen in Figure 3.8 and the torque can be seen in Figure

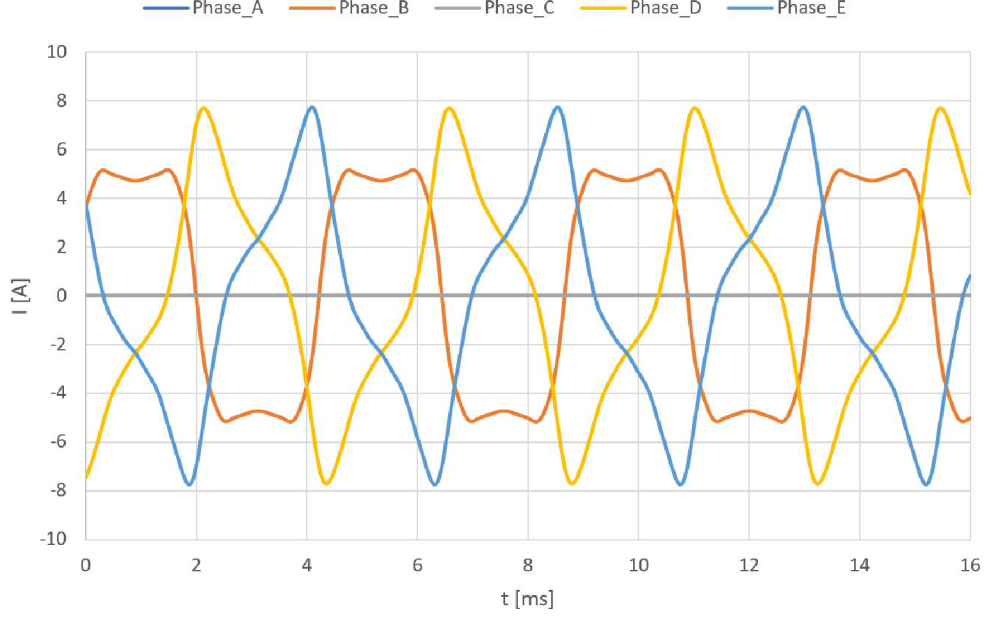


Figure 3.10: Reconfiguration two phases open (Phases A and C are open, 6 Nm).

3.9. The amplitude for phase B is 6.65 A, for phase D is 6.45 A and for phase 6.23 A (the amplitude of currents in normal state is 5 A).

Now take a look at optimization with 12 parameters. This optimization is based on knowledge, that the third harmonic currents are injected. This will change the equation (3.74 - 3.51) to:

$$I_A = I_{max1} \cos(\omega t + \varphi_1) + I_{max3} \cos(3\omega t + \varphi_3) \quad (3.57)$$

$$I_B = m_{b1} I_{max1} \cos(\omega t + \varphi_1 - 2\frac{\pi}{5} - \beta_{b1}) + m_{b3} I_{max3} \cos(3\omega t + \varphi_3 - 3\frac{2\pi}{5} - \beta_{b3}) \quad (3.58)$$

$$I_C = 0 \quad (3.59)$$

$$I_D = m_{d1} I_{max1} \cos(\omega t + \varphi_1 - 6\frac{\pi}{5} - \beta_{d1}) + m_{d3} I_{max3} \cos(3\omega t + \varphi_3 - 3\frac{6\pi}{5} - \beta_{d3}) \quad (3.60)$$

$$I_E = m_{e1} I_{max1} \cos(\omega t + \varphi_1 - 8\frac{\pi}{5} - \beta_{e1}) + m_{e3} I_{max3} \cos(3\omega t + \varphi_3 - 3\frac{8\pi}{5} - \beta_{e3}) \quad (3.61)$$

The third harmonic is used because it is creating an additional torque for the machine. As was mention in case of 6 parameters, for the 12 variables are 6 of them deduced to the amplitudes (including the third harmonic amplitudes) of currents and 6 for the phases shifts.

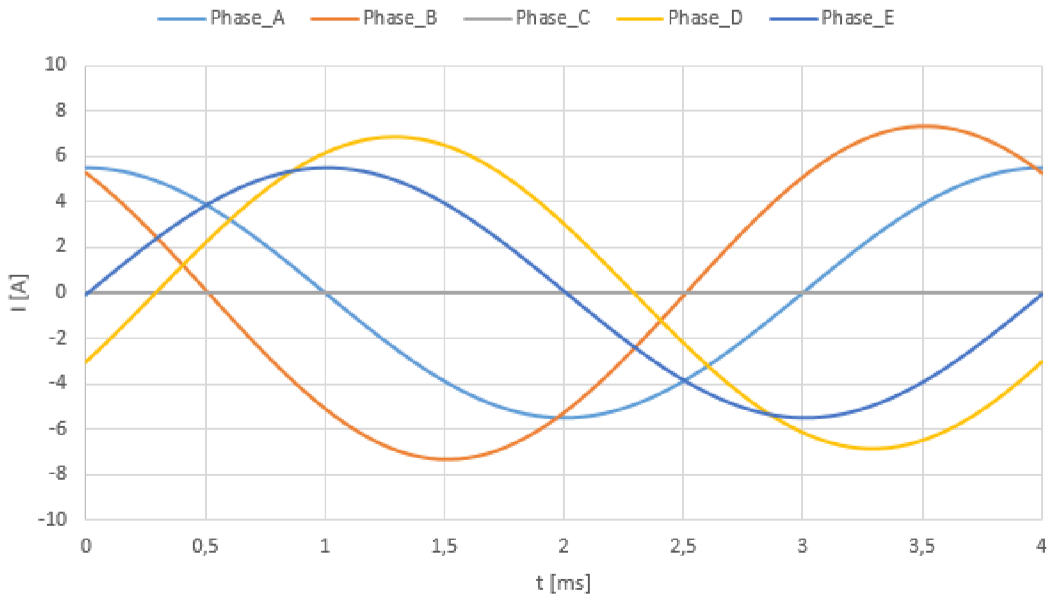


Figure 3.11: Curves of currents with application of GA(6 parameters).

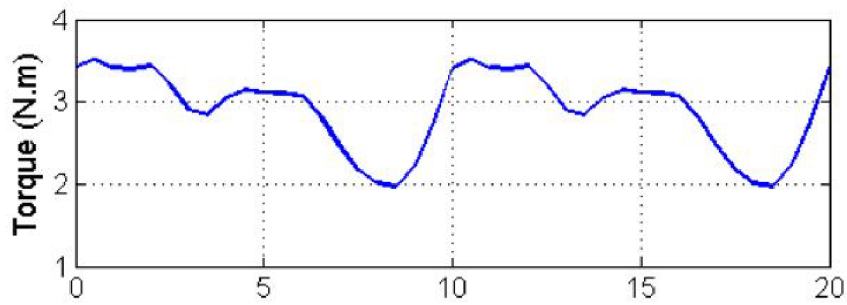


Figure 3.12: Torque with one phase open (6 parameters).

Table 3.2: Values of parameter using GA optimization(12 parameter fundamental) [30].

m_{b1}	m_{d1}	m_{e1}	β_{b1}	β_{d1}	β_{e1}
1.047	1.308	1.444	0.55	-0.481	0.008

Table 3.3: Values of parameter using GA optimization(12 parameters third harmonic) [30].

m_{b3}	m_{d3}	m_{e3}	β_{b3}	β_{d3}	β_{e3}
1.982	0.042	1.982	-1.524	-0.881	1.565

As can be seen from both Figures (3.8) and (3.9), the curve of the torque it is not ideal. The amplitudes and minimums differ from torque in normal operation. For the case of 6 parameters, the mean torque is 2.91 N.m, in case of 12 parameters the mean torque is equal to 2.98 N.m. If we compare the copper losses there are 36W for case of 6

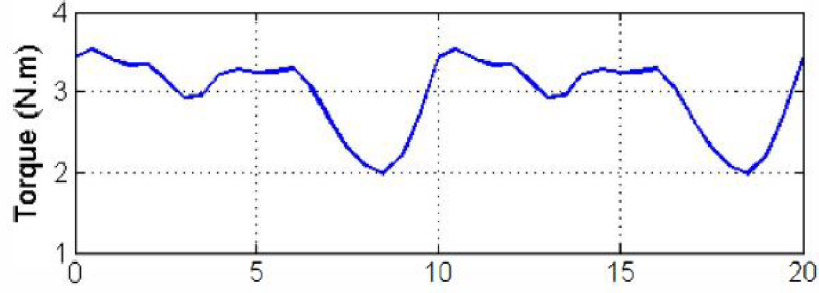


Figure 3.13: Torque with one phase open (12 parameters).

independent variables and 35.54W. Those values of copper losses are around 20 %, which is the maximum of the constrain for GA.

3.3.4 Different method of calculation currents On-line Optimal Current

This chapter will be based on [27], [33], [4] and [5]. There are many ways how to approach the problem of open-circuited. Model of permanent magnet synchronous machine (PMSM) can be created by equation (3.62):

$$v = Ri + l\left(\frac{di}{dt}\right) + e \quad (3.62)$$

In equation (3.62) v represents the vector of voltage, i represents current vector and e represents back electromotive force. Every one of these vectors is n -dimensional. Matrix of n -by- n inductance is represented by l . When we have the base equation the torque can be expressed as:

$$T = \varepsilon i \quad (3.63)$$

In equation (3.63) ε represent speed normalized back electromotive force vector. Based on (3.63) the reference current vector can be created. For the On-Line computation, an optimal condition has to be created. The criterion which is used is a minimum Joule losses. Similarly as in (3.35). By applying (3.63) to (3.35) the Joule losses are expressed such as :

$$P_{cu}(t) = \frac{RT^2}{\varepsilon^2} \quad (3.64)$$

$$i^* = A\varepsilon \quad (3.65)$$

As a first mode in [27] is normal operation of the machine. The machine is wye-connected. Because the machine is wye-connected, the currents can not have zero-

sequence components. To satisfy (3.65) the accessible EMF ε_{acc} have to be restricted.

$$\varepsilon_{acc} = \varepsilon - \varepsilon_z \quad (3.66)$$

$$\varepsilon_z = \left(\frac{\varepsilon_1 + \varepsilon_2 + \varepsilon_3 + \varepsilon_4 + \varepsilon_5}{\sqrt{5}} \right) \left(\frac{x_1 + x_2 + x_3 + x_4 + x_5}{\sqrt{5}} \right) \quad (3.67)$$

ε_z represents the zero-sequence component of ε . Now the criteria A can be calculated (3.68). The results of On-Line calculation for normal operation can be seen in Figure (3.11).

$$A = \frac{T^*}{\varepsilon_{acc}} \quad (3.68)$$

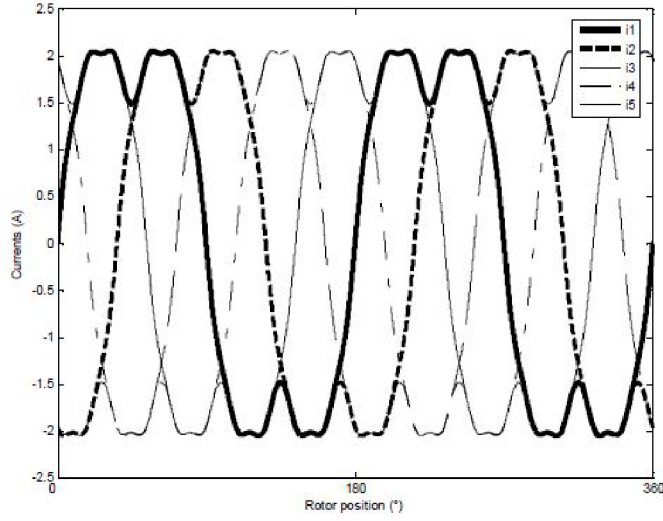


Figure 3.14: Optimal currents during normal operation.[27].

In cases of open phase circuited the accessible electromagnetic force vector needs to be recalculated with regards to the healthy number of phases. As an example will be shown for calculation, in the case of 2 open phases (phase 1 and 2 are open).

$$\varepsilon_{acc} = \varepsilon - \varepsilon_z - \varepsilon_{12} \quad (3.69)$$

$$\varepsilon_{12} = \varepsilon_1 x_1 - \varepsilon_3 x_3 \quad (3.70)$$

$$\varepsilon_z = \left(\frac{\varepsilon_3 + \varepsilon_4 + \varepsilon_5}{\sqrt{3}} \right) \left(\frac{x_3 + x_4 + x_5}{\sqrt{3}} \right) \quad (3.71)$$

In Figure (3.13) can be seen optimal current during one phase open-circuited with amplitude of 4 A. In Figures (3.14) the amplitudes are also 4 A, but for each phase.

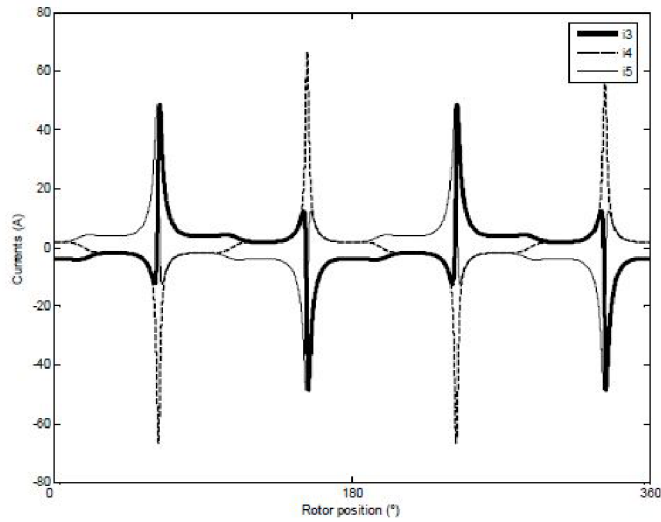


Figure 3.15: Optimal currents during open-phase circuited(one phase open).[27].

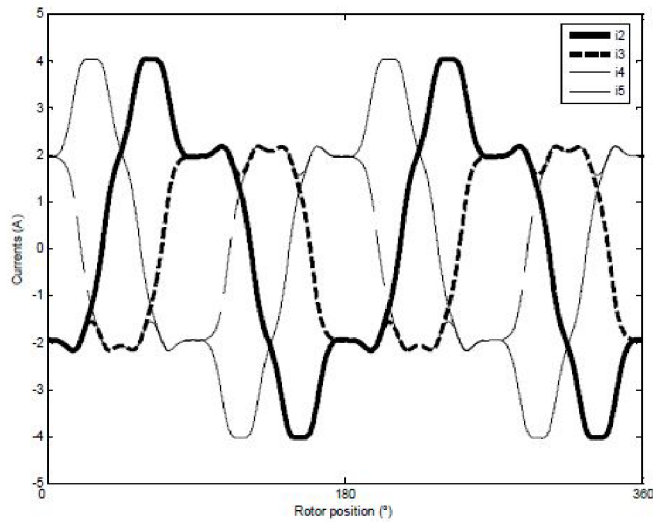


Figure 3.16: Optimal currents during open-phase circuited(one phase open).[27].

Table 3.4: Values of torque in each of the open phase scenarios(On-Line method).

-	5 phases	4 phases	3 (consecutive) phases	3 (non-consecutive) phases
Torque [N.m]	2	1.71	0.449	1.49

If we take a look at the torque values for each mode, the values have to decrease under the condition of keeping the Joule losses around the value of normal operation(32.3 W). In Table (3.4) are values of torque for the normal and open-phase operation. If we compare the values, in case of one open phase the torque is down 14.5%.

Now we can compare the Joule losses in each scenario. In Table (3.5) can be seen all values of Joule losses in each mode of operation for the machine. In the case of one phase

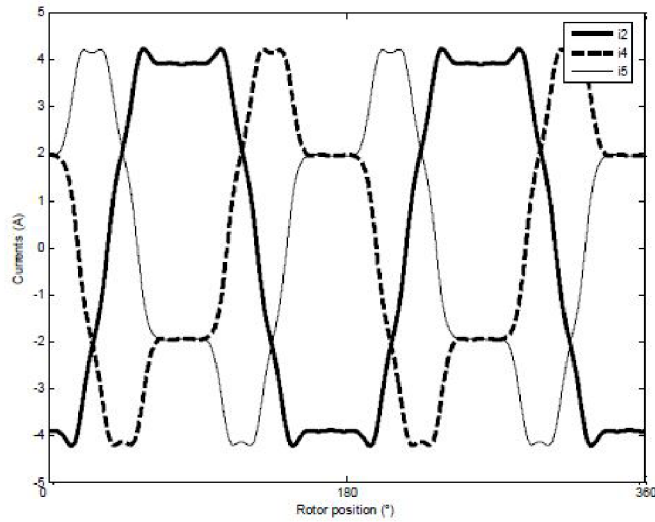


Figure 3.17: Optimal currents during open-phase circuited(two non-consecutive phase open) [27].

open, the Joule losses differ around 36% (the losses are higher than in normal operation). In the case of two open phases which are non-consecutive, the Joule losses have grown to a value of 58 W. Which mean increase of 79.6% compared to the normal operation. As last is the case of open phase circuited with two consecutive phases. In this scenario, the Joule losses obtain value of 641 W. This value of Joule losses represents an increase of 1884% compared to the normal operation.

Table 3.5: Values of Joule losses in each of the open phase scenarios(On-Line method).

-	5 phases	4 phases	3 (consecutive) phases	3 (non-consecutive) phases
P_{cu} [W]	32.3	44	641	58

4 Extended analysis by means of fine element methods

In this chapter, a model of the machine is created for the testing purposes. This model is base on [34]. This motor was created with fractional-slot concentrated wing on stator. In rotor there are interior permanent magnets. All calculation are done in software Ansys Maxwell 2D. Because is used a single layer winding and as can be seen from Table 2.1 concentrated winding is used. Also, it can be seen from Table 2.2 it is stable winding (balanced winding). The ration of stator slots and rotor poles should be [22], [35]:

$$Q = 2mk \quad (4.1)$$

$$2p_r = Q \pm k \quad (4.2)$$

Where Q represents the stator slot number, p_r represents the number of rotor pole-pair and k have a condition that it has to be an even integer to evade unbalance force. The number of stator slots has been pick as 20 a rotor pole-pair to 9. Parameters of the motor can be seen in Table 4.1.

Table 4.1: Parameters of the motor.

Parameters	Values
Rated Power [W]	2000
Rated Voltage [V]	100
Rated speed [r/min]	1500
Number of stator slots [-]	20
Number of rotor pole-pair [-]	9
Stator outer radius [mm]	70
Stator inner radius [mm]	42.75
Rotor outer radius [mm]	42.15
Rotor inner radius [mm]	28.8
Air gap length [mm]	0.6
Thickness of PM [mm]	2
Width of PM [mm]	12

By the parameters which are in Table 4.1 the IPM motor has been modelled. The whole model will be analyzed in the 2D FEA. Sheets for the motor are M470-30A and N33UH magnets. Geometry of the motor can be seen in Figure 4.1. Each phase has its

colour. Phase A have a blue colour, phase B has brown colour, phase C yellow, phase D orange and phase E have black colour.

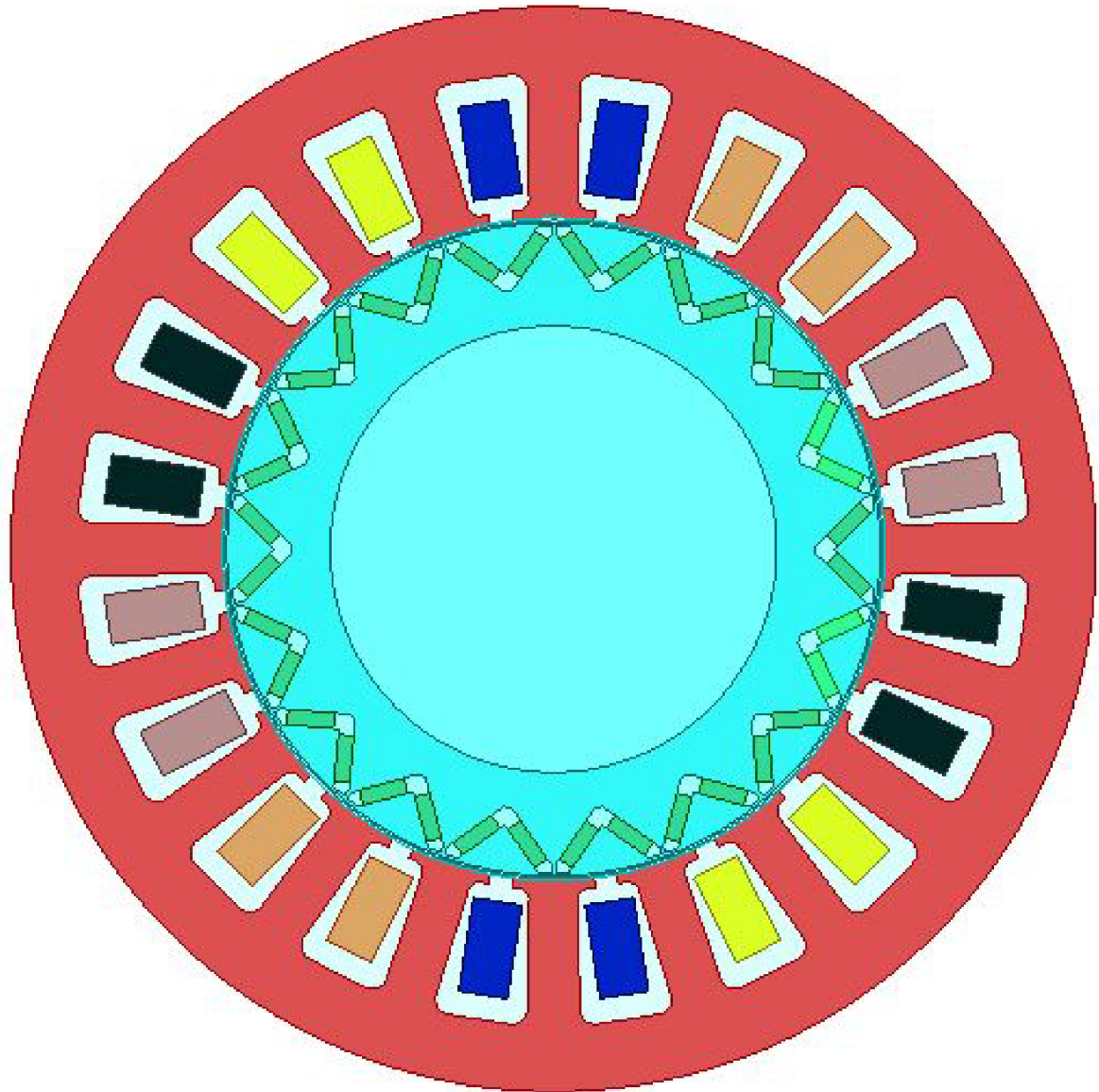


Figure 4.1: Geometry of the motor.

The motor as it was mentioned earlier FEA will be applied, that means the mesh of the machine needs to be generated. The maximum element of the air-gap is 0.3 mm, for the rotor is 3 mm for an element and 3.5 mm for the stator. Generated mesh for the machine can be seen in Figure 4.3.

4.1 Motor under no-load

In this chapter, the motor is tested under no-load. From this testing, we can get back EMF to correctly calculate the curves of currents for each phase. In Figure 4.2 can be seen the back EMF.

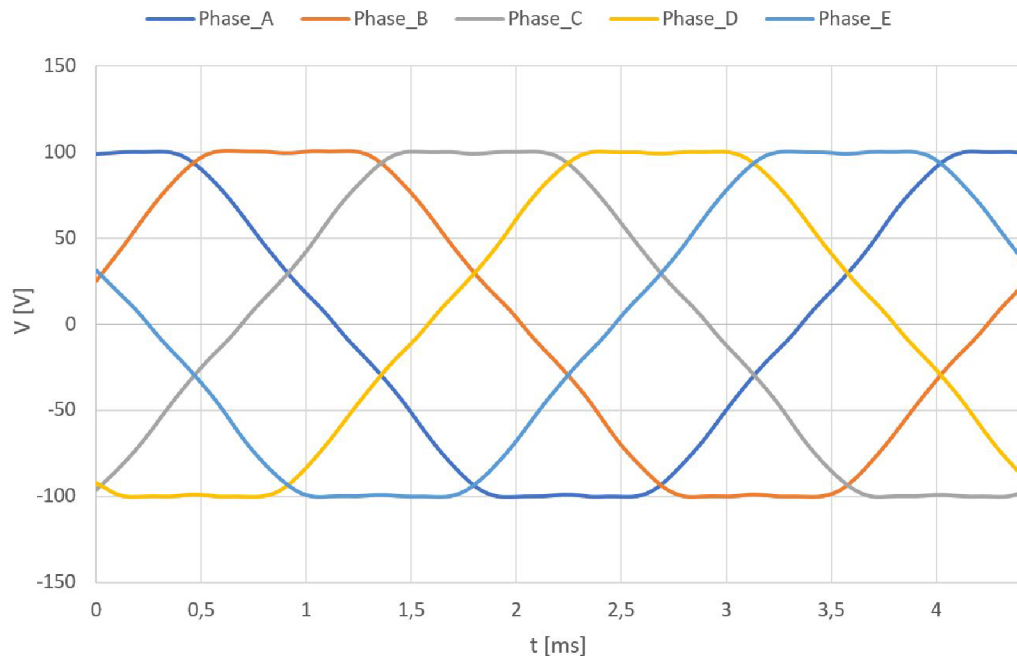


Figure 4.2: Back EMF(no-load).

As can be seen from Figure 4.2 the back EMF is not perfectly sinusoidal and because of that, the currents in case of open-phase circuited will differ. Both cases will be mentioned in the chapter 4.2. As next it can be shown the magnetic induction in the model. The values of magnetic induction can be seen in Table 4.2. The maximal magnetic induction is in the rotor bridge and it reaches 2.18 T. In other places the values of magnetic induction are in the range of 1.1 to 1.3 T.

Table 4.2: Measured maximal values of magnetic induction of the motor

place	B [T]
Stator yoke	1.10
In stator tooth	1.19
In head of tooth	1.21
Rotor yoke	1.16
Rotor bridge	2.18

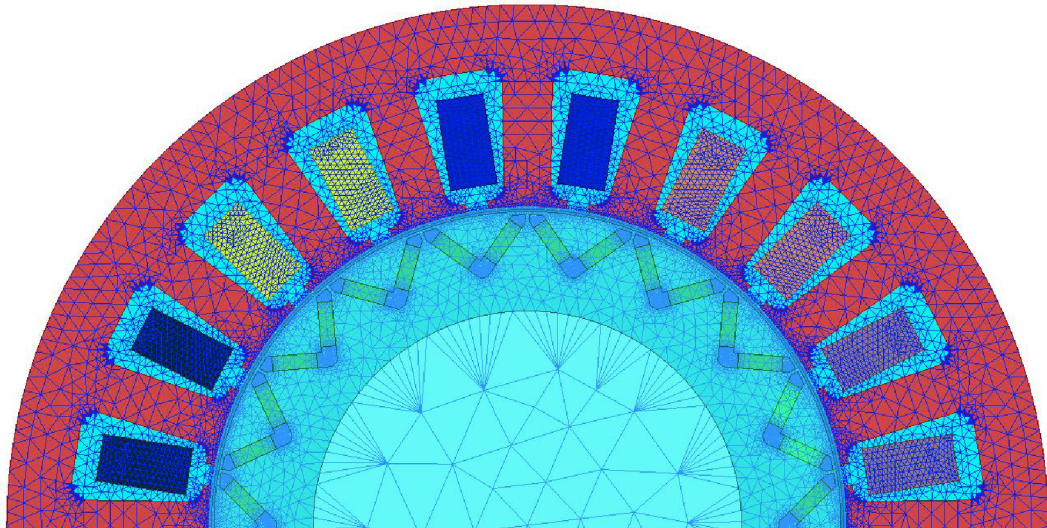


Figure 4.3: Mesh of the half of the motor.

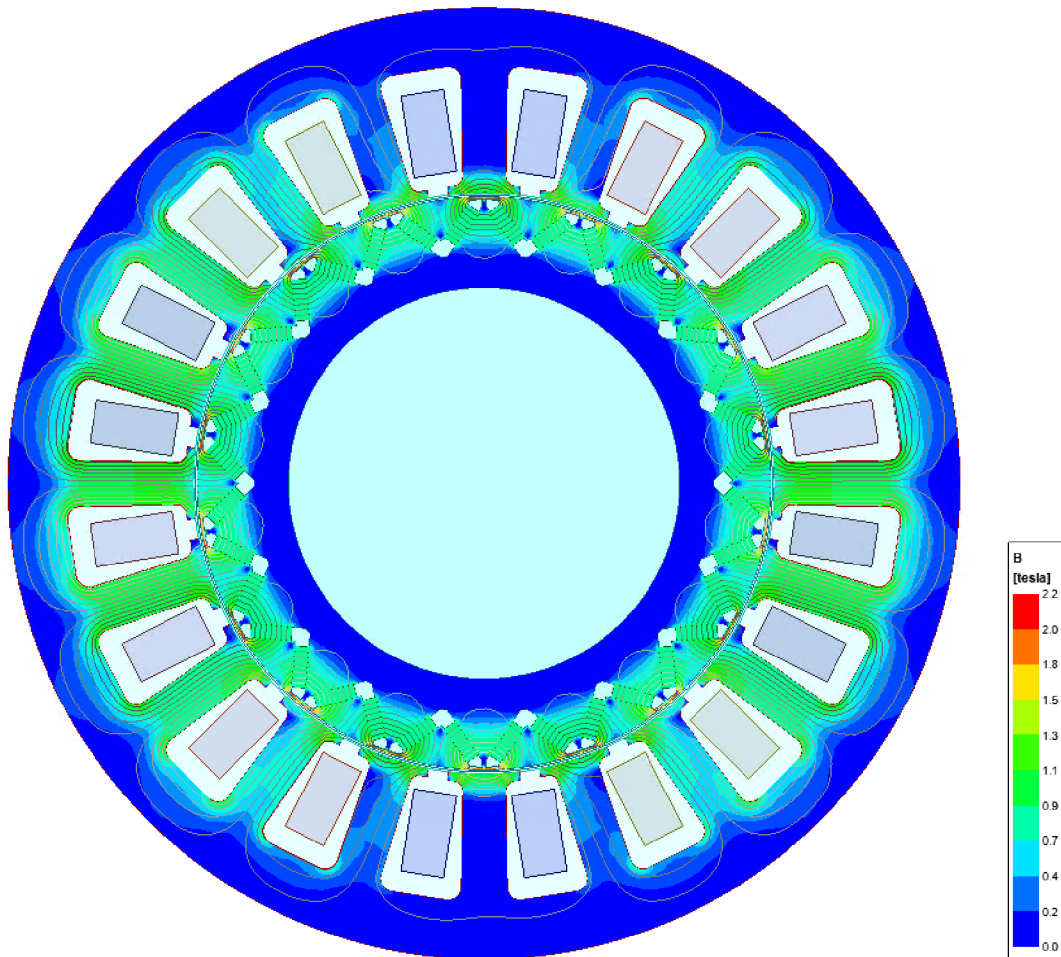


Figure 4.4: Induction under no-load.

4.2 Motor under full-load

As in was mentioned in the chapter 4.1. The back EMF in the motor Fig. 4.1 is not sinusoidal because of that, two possible solutions can be made for the case of full load. One is to use currents which were calculated with perfectly sinusoidal back EMF with the amplitude of 100 V, or use the measured back EMF with FEA. In both cases, the target torque is 10 N.m.

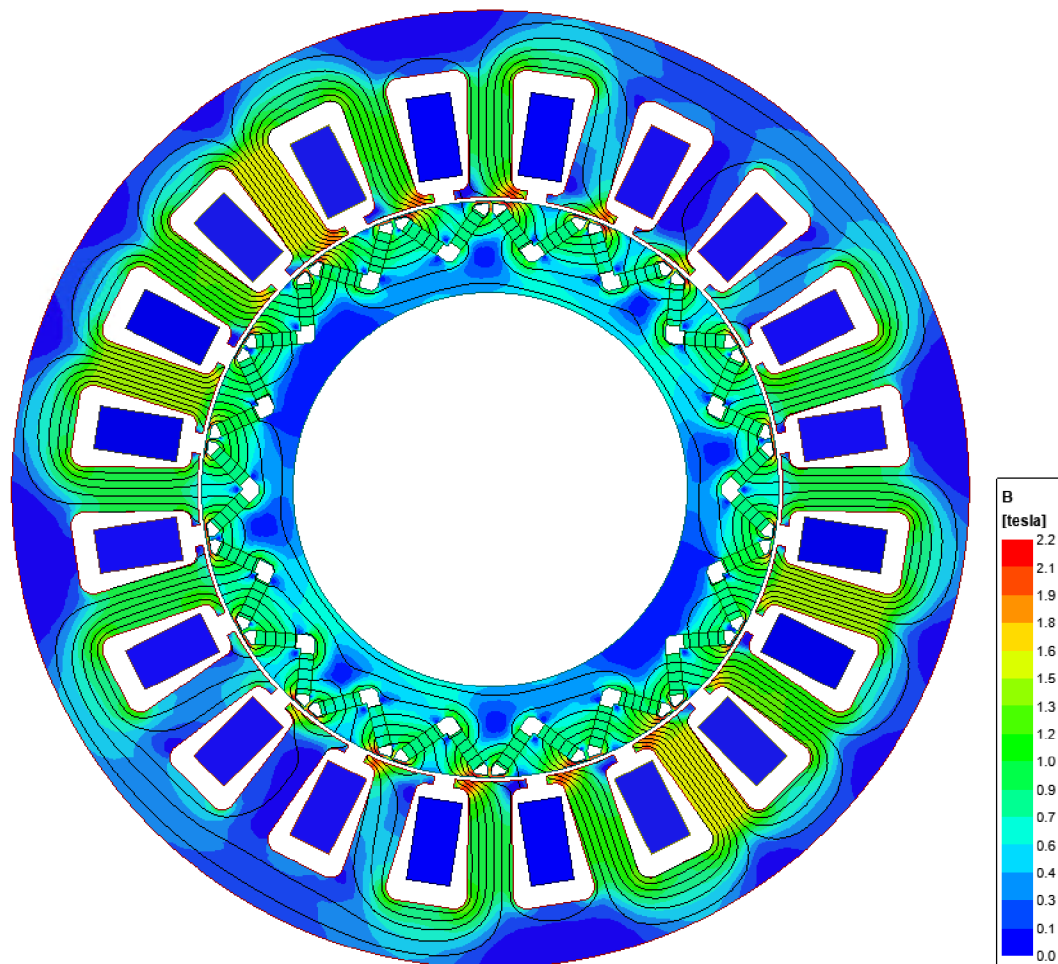


Figure 4.5: Magnetic induction full-load.

4.2.1 Sinusoidal back EMF

In Figure 4.5 can be seen current in all phases of the motor. This current was based on sinusoidal back EMF with an amplitude of 100 V. With this, the amplitude of current for each phase is 5 A. When the analyzed the torque is the primary calculated to see if the model of current correctly calculated.

The calculated torque can be seen in Figure 4.6. The value of the mean torque is 8.41 N.m, which is 16 % lower than the reference torque. As can be seen from Figure 4.5 and

4.6 the target torque was not met. With this curve of currents would need to be a higher amplitude to achieve the required torque.

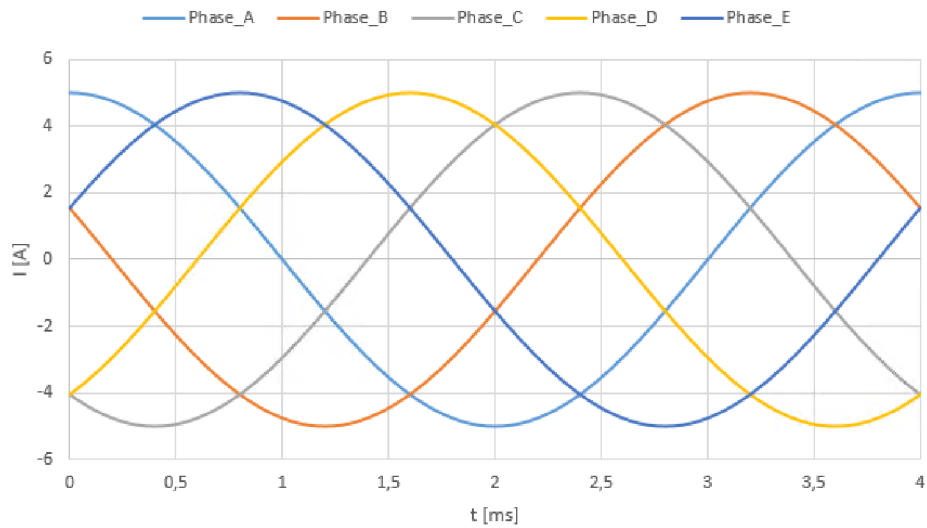


Figure 4.6: Currents (Sinusoidal back EMF).

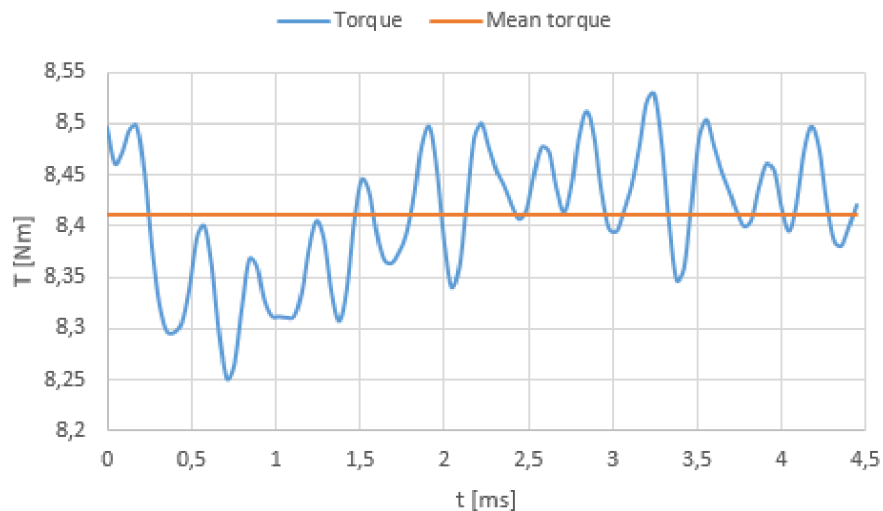


Figure 4.7: Torque 1500 rpm (sinusoidal back EMF).

4.2.2 Back EMF from no-load

In Figure 4.7 are currents which are calculated with regards to back EMF which is calculated in no load. The amplitude of currents in each phase are 5.6 A. with this current is the mean torque 10.1 N.m. This torque can be seen in Figure 4.8. With this calculation the torque wanted and torque calculated are just 1%. It also needs to be point out, that the amplitudes differ, and it would be possible even with sinusoidal back EMF configuration to create 10 N.m of torque.

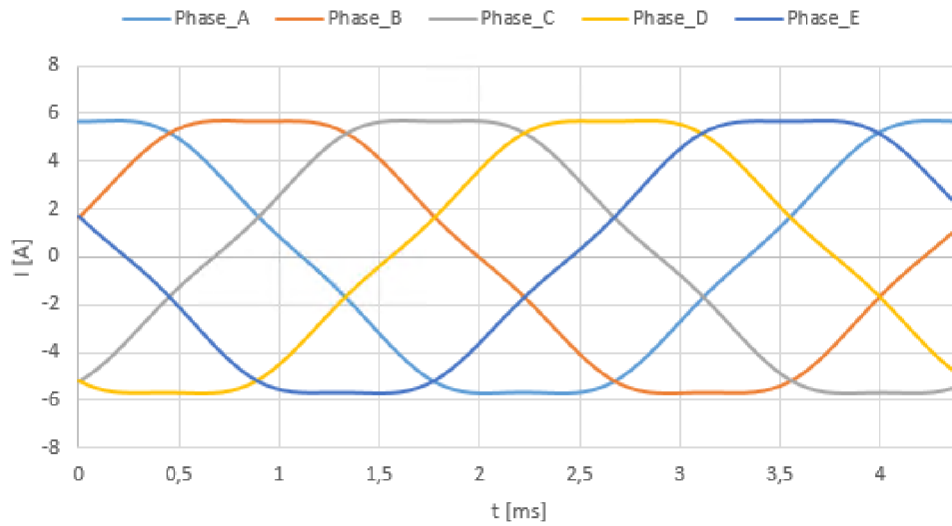


Figure 4.8: Currents (no-load back EMF)

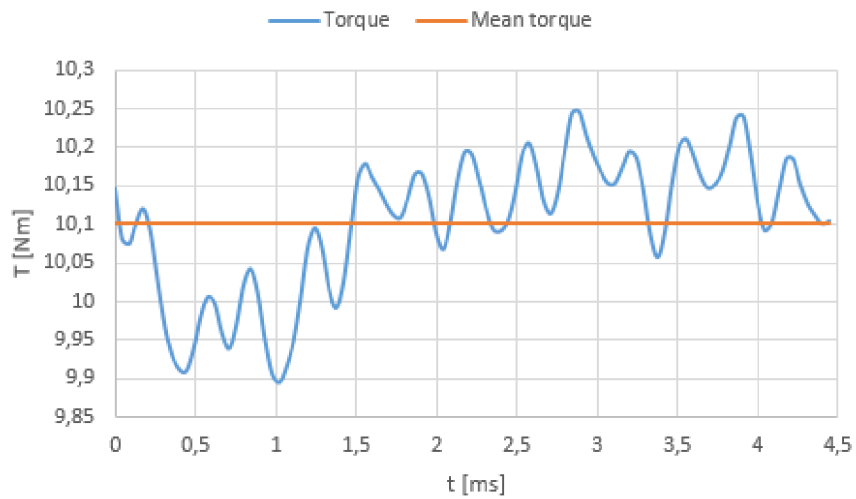


Figure 4.9: Torque 1500 rpm (no-load back EMF).

Table 4.3: Calculated maximal values of magnetic induction of the motor (Full-load).

place	B [T]
Stator yoke	1.20
In stator tooth	1.50
In head of tooth	1.92
Rotor yoke	1.35
Rotor bridge	2.20

The maximal magnetic induction was in the same place as in no-load (rotor bridge). The value of magnetic induction 2.20 T. The magnitude of the rest of magnetic induction

in the motor parts is the range of 1.20 to 1.95 T. The maximal values in either place can be seen in Table 4.3.

In the next steps, the reconfiguration will be used with measured values of back EMF and also the wanted torque will decrease for each case.

4.3 One phase open

In this case, as it was mentioned earlier, the torque will be decreased to keep the Joule losses relatively low. The value of torque will be 8 N.m. It is 20 % lost of torque but it is still quite good (the motor can still function). In Figure 4.10 the curves of currents for each phase. But as a first example, there is a reconfiguration for the full torque. The amplitudes for phases are the same as in chapter 3.3.2 for case on one-phase open. Curves of currents can be seen in Figure 4.11.

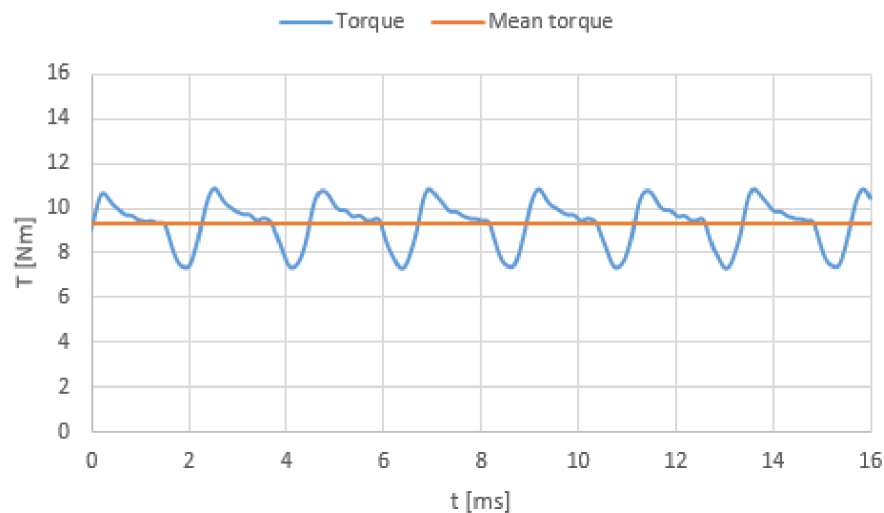


Figure 4.10: Torque 1500 rpm (one phase open, 10 Nm).

The maximal amount of torque was 10.6 Nm and the lowest point was 7.6 Nm. Overall, the average torque in the motor was 9.4 Nm which is 6 % off the target value of 10 Nm of torque.

Now the torque required is lowered to 8 Nm. The calculation was run again. The currents just changed in amplitudes. Current with the produced torque can be seen in Figures 4.12 and 4.13. The average torque is 7.6 Nm. Which is just shy of 5 % from the required torque of 8 Nm.

In total compared to normal operating case it is 76 % of nominal torque. This percentage could be increased with and additional constraints. As an example, the amplitudes of phases C and E. These values could be kept at least on value as in normal mode, or get a better look on redistribution of current in each phase. But these are not the only possible ways to achieve better results. The change could be made in the motor itself.

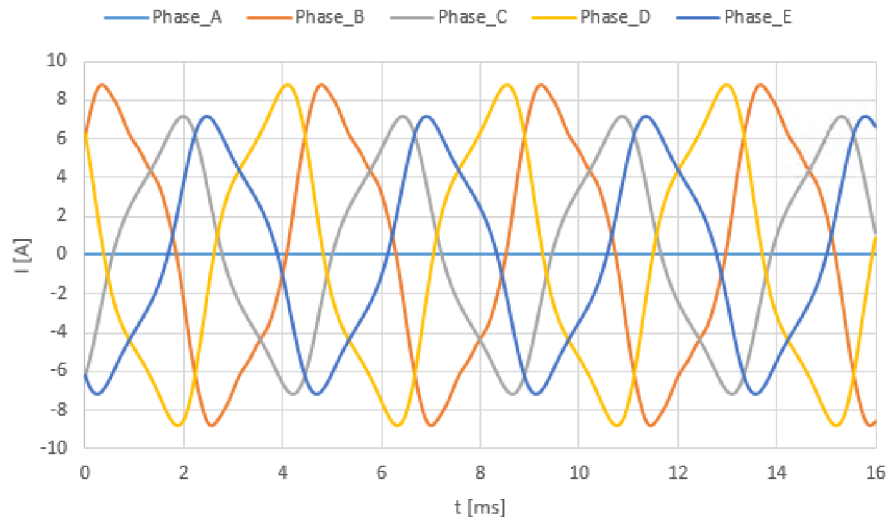


Figure 4.11: Currents (one phase open, 10 Nm).

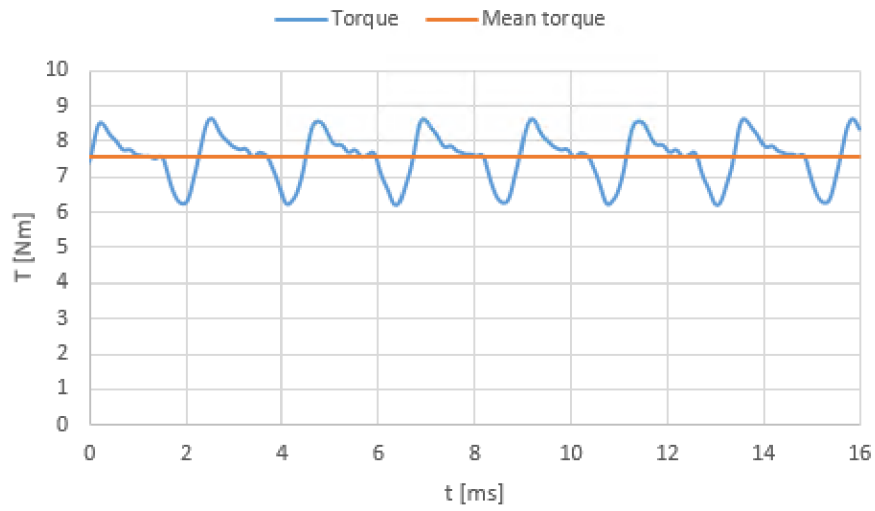


Figure 4.12: Torque 1500 rpm (one phase open, 8 Nm).

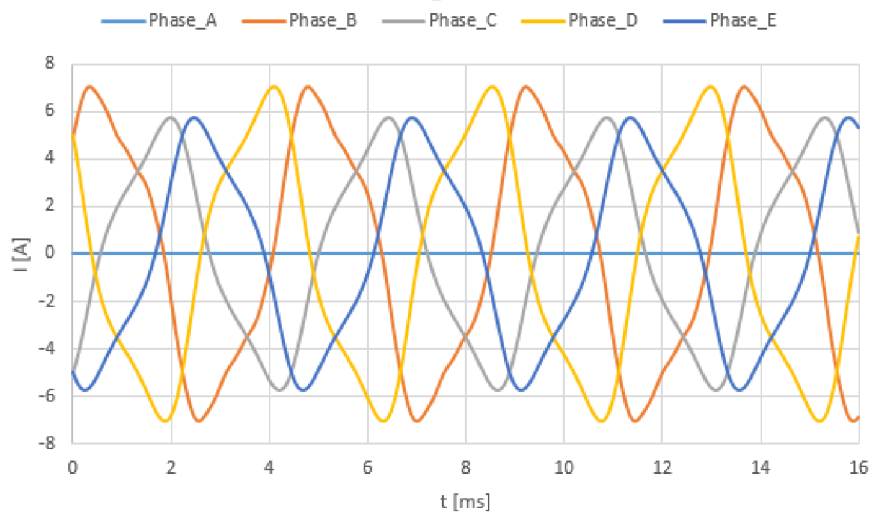


Figure 4.13: Currents (one phase open, 8 Nm).

4.4 Two phases open

At the start of this chapter needs to be sad there will be just one of them will be mentioned and that will be the case of non-consecutive phases. Case of consecutive phases. For the non-consecutive, the curves of the currents can be seen in Figure 4.14. The amplitudes of currents are mentioned in chapter 3.3.2. According to the current, the torque can be seen in Figure 4.15. The average value of the torque was 5.6 Nm. Which is 7 % lower than the required torque of 6 Nm. In total it is 56 % of the nominal torque (nominal torque is 10 Nm). To achieve the required/wanted torque, it would be needed to change the values of amplitudes. This could have been done with more constraints. With 3 out of 5 phases is possible to continue the function of the motor, but with this reconfiguration is possible to achieve with this motor just 56 %. But it is necessary to mention that the amplitudes are not that high and would not generate that much higher Joule losses.

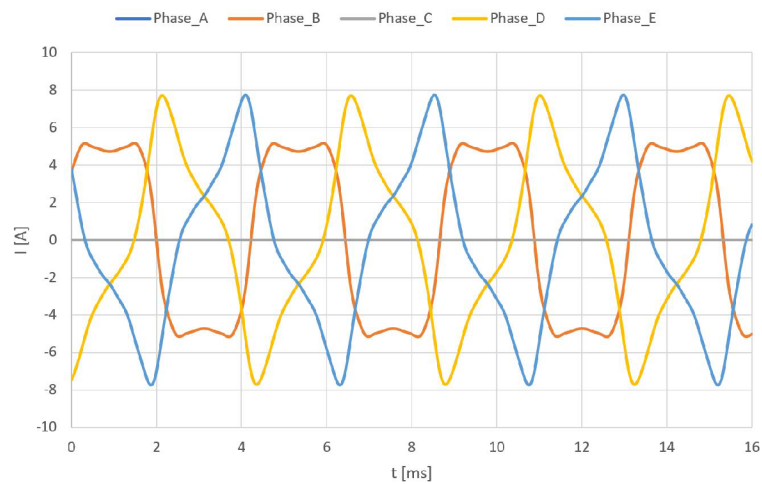


Figure 4.14: Currents (two phases open, 6 Nm).

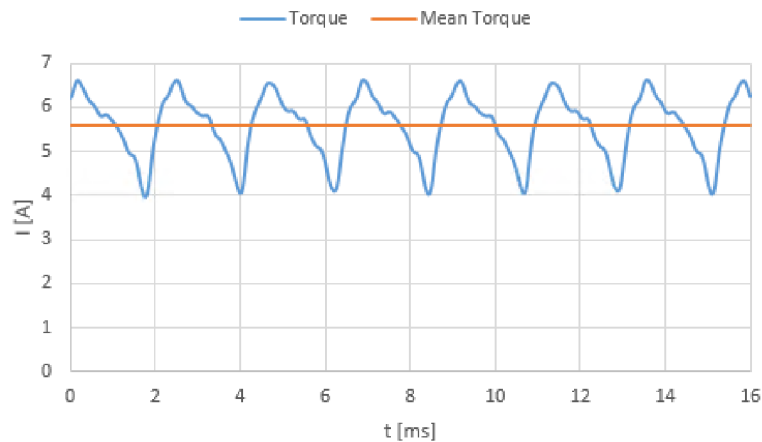


Figure 4.15: Torque 1500 rpm (one phase open, 8 Nm).

Conclusion

This master thesis deals with poly-phase machines as a whole. In the first part of this thesis, there are mentioned way how to operate (control) the poly-phase machine, for example, five-phase machine. As well as the controlling of the machine there are multiple arrangements describe for the machine. At the end of the first chapter is to describe a few ways how to test the poly-phase machines by using back-to-back testing, two frequency method or inverter-driven method.

In the second part of this thesis is to describe a comparison of the five-phase machine to the three-phase machine. Also, there are tables for five as well as for three-phase machine in which are describe their balance and recommended winding for the number of slots and poles.

In the third part there is describe the mathematical model of the five-phase permanent magnet machines. This model has an injection of the third harmonic to achieve a higher value of torque. This can be seen from equation 3.29. As the next step, there is an equation for the short circuit of the five-phase machine. These equations are for the cases of one or two phases in short circuit. In the last part of this chapter is the state of the machine with open-circuit. Three ways are mentioned and those are Genetic algorithm, On-Line optimal current and Lagrange multipliers. Every one of the reconfiguration is looked at, but The Lagrange multipliers are closely described. For Lagrange multipliers are two constraints are created. One of the constrain is that the sum of the currents is equal to zero and the second one is that the power wanted is equal to the power output. With this constrains are the LM calculated and final equation for the currents created. After the equation was created there was a test to create the output torque of 10 Nm with perfectly sinusoidal back EMF.

The result of this calculation can be seen in Figure 3.4. The amplitudes of each phase was 5.5 A. After the calculation for normal operation, the first case of open phase was calculated. In case of one-phase open the amplitudes of phases B and E were 8.75 A and for phases C and D 7.1 A. This was 1.59 times higher then in normal operation, for the phase C this value was 1.29 times. This values are to achieve a 10 Nm of torque. If the requirement for the torque is lower to 8 Nm (20 % lower), the amplitudes will decrease. This value of torque was picked because in case of one-phase open there are four out of five phases in function therefore the output should by lowered about the 20 %. Same it goes in the case of two-phase open. In this scenario, there are two possible outcomes. One in the case of consecutive phases are open and the second one the phases are non-consecutive. As first it was looking at the consecutive scenario. In this case, the amplitudes for currents to achieve 10 Nm of torque were from 3 to 4 times higher than in normal operation. But as it was mentioned the torque should be lowered to 6 Nm. When the torque is lowered to 6 Nm of torque the amplitude if phase D is at 12.8 A and

amplitudes of phases C and E are at 9.8 A. These values are high and it would need to be counted on this fact in the design of the machine. In case of two non-consecutive phase, the amplitudes for phases D and E are 7.6 A and for phase B is 5.1 A.

All of this curves has been input for the FEA and the results of the analyze is mentioned in the last chapter. This was created to approve the method. In case of one phase open the average torque was 7.6 Nm and therefore the result it is not 80 % but 76 % of the nominal torque. For the case of two non-consecutive phases open the average torque was 5.6 Nm, which is 56 % of the nominal torque. These values could be increased by applying more constrains. This mean more LM. Also, the model was base on the model which mean the design is not the same and for that reason, the design could be improved to achieve better results of output torque.

References

- [1] T.J.E. Miller J.R. Hendershot Jr. *Design of Brushless Permanent-Magnet Machines*. 102 Triano Circle: Motor Design Books LLC, 2010. ISBN: 9780984068708.
- [2] F. Labrique E. Matagne D. Telteu F. Baudart B. Dehez and P. Alexandre. *Control strategy with minimal controller reconfiguration of fault tolerant polyphase PMSM drives under open circuit fault of one phase*. Tech. rep. ICEM 2010, Rome, 2010.
- [3] Leila Parsa Ali Mohammadpour Siavash Sadeghi. *A Generalized Fault-Tolerant Control Strategy for Five-Phase PM Motor Drives Considering Star, Pentagon, and Pentacle Connections of Stator Windings*. Tech. rep. Department of Electrical, Computer, and Systems Engineering, Advanced Technology Center, General Motors Company, 2013.
- [4] Hamid A. Toliyat Leila Parsa. "Fault-Tolerant Interior-Permanent-Magnet Machines for Hybrid Electric Vehicle Applications". In: *IEEE TRANSACTIONS ON VEHICULAR TECHNOLOGY* 56.4 (2007). ISSN: 0018-9545.
- [5] Leila Parsa Suman Dwari. "An Optimal Control Technique for Multiphase PM Machines Under Open-Circuit Faults". In: *IEEE TRANSACTIONS ON INDUSTRIAL ELECTRONICS* 55.5 (May 2008). ISSN: 0278-0046.
- [6] L. Livadaru Al. Simion R. Outbib A.M. Mihai S. Benelghali. "FEM Analysis upon Significance of Different Permanent Magnet Types Used in Five-Phase PM Generator fro Gearless Small-Scale Wind". In: (2012). ISSN: 978-1-4673-0142.
- [7] Pizza A. Del Pizzo A. Di Noia L.P. "Five-Phase Permanent-Magnet Motor". In: *IEEE TRANSACTIONS ON INDUSTRIAL ELECTRONICS* (2017). ISSN: 978-8-8872-3730-6.
- [8] AKM Arafat Seungdeog Choi Sai Sudheer Reddy Bonthu Md. Zakirul Islam. "Five-phase External Rotor Permanent Magnet Assisted Synchronous Reluctance Motor for In-wheel Applications". In: *IEEE TRANSACTIONS ON INDUSTRIAL ELECTRONICS* (2017). ISSN: 978-1-5090-3953-1.
- [9] Hamid A. Toliyat Leila Parsa. "Five-Phase Permanent-Magnet Motor". In: *IEEE TRANSACTIONS ON INDUSTRIAL ELECTRONICS* 41.1 (2005). ISSN: 0093-9994.

- [10] S. Siddiqui A. Nigam. "Modeling and simulation of five-phase permanent magnet synchronous motor". In: *VSRD Technical Non-Technical Journal* 1 (2010).
- [11] L.F. Gonzalez J.Y. Hung. "On parallel habrid-electric propulsion system for un-manned aerial vehicles". In: *Progress in Aerospace Sciences* 51 (May 2012).
- [12] A.T. Isikveren C.Pornet. "Conceptual design of hybrid-electric transport aircraft". In: *Progress in Aerospace Sciences* 79 (2015).
- [13] Seungdeog Choi Sai Sudheer Reddy Bonthu Jeihoon Baek. "Comparison of Optimized Permanent Magnet Assisted Synchronous Reluctance Motors with Three-phase and Five-phase Systems". In: *IEEE Energy Conversion Congress and Exposition* 79 (2014).
- [14] H. A. Toliyat Y. Deshpande. "Design of an outer rotor ferrite assisted synchronous reluctance machine (Fa-SynRM) for electric two wheeler application". In: *IEEE Energy Conversion Congress and Exposition* 3147-3154 (2014).
- [15] S. Choi S. S. R. Bonthu. "Design procedure for multi-phase external rotor permanent magnet assisted sychronous reluctance machines". In: *IEEE Applied Power Electronics Conference and Exposition* 1131-1137. (2016).
- [16] Harizan Che Mat Haris Mohd Syazimie Bin Zulkifli Wan Noraishah Binti Wan Abdul Munim. *Five Phase Space Vector Modulation Voltage Source Inverter Using Large Vector Only*. Tech. rep. Universiti Teknologi MARA, Faculty of Electrical Engineerin, 2012.
- [17] Alberto Tassarolo. *On the modeling of Poly-Phase Electric Machines throught Vector-Space Decomposition: Numeric Application Cases*. Tech. rep. University of Trieste, Electrical, Electronic and Computer Engineering Department, 2009.
- [18] Alberto Tassarolo. *On the modeling of Poly-Phase Electric Machines throught Vector-Space Decomposition:Theoretical Considaration*. Tech. rep. University of Trieste, Electrical, Electronic and Computer Engineering Department, 2009.
- [19] Jorma Luomi. *Transient Phenomena in Electrical Machines*. Goteborg, 1998.
- [20] Martin Jones Mikel Zabaleta Emil Levi. *Regenerative Testing of Multiphase Machines with Multiple Three-phase Windings*. Tech. rep. Liverpool John Moores University, Ingeteam Power Technology, 2018.
- [21] Masahiro Shoji Yongjae Kim Hideo Dohmeki Makoto Yoneda. *Novel Selection of the Slot/Pole Ratio of the PMSM for Auxiliary Automobile*. Tech. rep. Oriental Motor co.,ltd, Musashi Institute of Technology, 2006.
- [22] Valéria Hrabovcová Juha Pyronen Tapani Jokinen. *Design Of Rotating Electrical Machines*. Second Edition. West Sussex: John Wiley Sons, Ltd, 2014. ISBN: 978-1-118-58157-5.

- [23] Luís F. A. Pereira Ricardo S da Rosa Luís A. Peeira Sérgio Haffner. *Performance Comparison of Five Phase and ThreePhase Induction Machines under Steady State including Losses and Saturation*. Tech. rep. Federal University of Rio Grande do Sul, Electrical Engineering Graduate Program, 2013.
- [24] Hamid A. Toliyat Leila Parsa. “Multi-Phase Permanent Magnet Motor Drives”. In: *IEEE TRANSACTIONS ON INDUSTRIAL ELECTRONICS* 67.1 (2003). ISSN: 0-7803-7883-0.
- [25] Thomas A. Lipo Hamid A. Toliyat Shailesh P. Waikar. *Analysis and Simulation of Five-Phase Synchronous Reluctance Machines Including Third Harmonic of Airgap MMF*. Tech. rep. University of Wisconsin, 1998.
- [26] M. Gabsi I. Slama-Belkhodja E. Ben Sedrine J. Ojeda. *Reference Currents Reconfiguration of a Five-Phase Flux Switching Machine To Improve the Operation under Short-Circuit Phase Faults*. Tech. rep. Université de Tunis El Manar, 2011.
- [27] Y. Crévits X. Kestelyn E. Semail. *Generation of On-line Optimal Current References for Multi-phase Permanent Magnet Machines with Open-circuited Phases*. Tech. rep. Univ Lille Nord de France, 2009.
- [28] Patrick L. Chapman Alan P. Wu. *Simple Expressions for Optimal Current Waveforms for Permanent-Magnet Synchronous Machine Drives*. Tech. rep. Northrop Grumman Space Technology, University of Illinois at Urbana-Champaign, 2005.
- [29] Leila Parsa Ali Mohammadpour. “Global Fault-Tolerant Control Technique for Multiphase Permanent-Magnet Machines”. In: *IEEE TRANSACTIONS ON INDUSTRY APPLICATIONS* 51.1 (2015). ISSN: 0093-9994.
- [30] I. Slama-Belkhodja M. Gabsi E. Ben Sedrine J. Ojeda. “Five-Phase Flux Switching Machine: Optimal current waveforms in order to improve open phase operation”. In: (2012). ISSN: 978-1-4673-2421.
- [31] Hideo Yamashita Norio Kowata Vlatko Čingoski Kazufumi Kaneda. “Inverse Shape Optimization Using Dynamically Adjustable Genetic Algorithms”. In: (1999). ISSN: 0885-8969.
- [32] R. Wrobel M. Lukaniszyn M. Jagieła. “Optimization of Permanent Magnet Shape for Minimum Cogging Torque Using a Genetic Algorithm”. In: (2004). ISSN: 0018-9464.
- [33] Hamid A. Toliyat. “Analysis and Simulation of Five-Phase Variable-Speed Induction Motor Drives Under Asymmetrical Connections”. In: *IEEE TRANSACTIONS ON POWER ELECTRONICS* 13.4 (1998). ISSN: 0885-8993.

- [34] Robert D.Lorenz Ademir Nied Ming Cheng Li Zhang Ying Fan. “Design and Comparison of Three-Phase and Five-Phase FTFSCW-IPM Motor Open-End Winding Drive Systems for Electric Vehicles Applications”. In: *IEEE TRANSACTIONS ON VEHICULAR TECHNOLOGY* 67.1 (2018). ISSN: 0018-9545.
- [35] Wenxiang Zhao Longgang Sun Mingming Shao Zhengmeng Liu Qian Chen Guohai Liu. “Design and Comparison of Two Fault-Tolerant Interior-Permanent-Magnet Motors”. In: *IEEE TRANSACTIONS ON INDUSTRIAL ELECTRONICS* 67.1 (2014). ISSN: 0278-0046.